

ONLINE PROCESS MONITORING OF PART  
MANUFACTURING USING MVA

ONLINE PROCESS MONITORING  
OF DISCRETE PART MANUFACTURING  
USING MULTIVARIATE ANALYSIS

By

HOLLY DZUBA, B.Eng.Mgmt.

A Thesis

Submitted to the School of Graduate Studies

in Partial Fulfilment of the Requirements

for the Degree

Master of Applied Science

McMaster University

© Copyright by Holly Dzuba, November 2010

MASTER OF APPLIED SCIENCE (2010)

McMaster University

(Mechanical Engineering)

Hamilton, Ontario

TITLE: Online Process Monitoring of Discrete Part  
Manufacturing Using Multivariate Analysis

AUTHOR: Holly Dzuba, B.Eng.Mgmt. (McMaster University)

SUPERVISOR: Professor S.C. Veldhuis

NUMBER OF PAGES: xii, 121

## **Abstract**

The significance of online process monitoring of discrete part manufacturing using multivariate analysis is its ability to help the Canadian manufacturing industry compete in the global market. Process monitoring can accomplish this by: assessing the state of a machining system for unusual occurrences, moving the part quality prediction upstream, and producing higher volumes of in specification parts for improved profits.

The focus of this research was discrete process monitoring of a turning operation in a laboratory at the McMaster Manufacturing Research Institute (MMRI) and an industrial machining cell at Glueckler Metal Incorporated (GMI). Both applications involved instrumentation of a lathe with current sensors, an accelerometer and thermocouples. Serial port communication between the machine control panel and computer was established to allow for online automated data acquisition. The multivariate latent model applied was principal component analysis to develop correlations among the machining process information. Principal component analysis was successful in identifying the occurrence of an out of balance spindle, unusual surface finish, changes in depth of cut, and a worn tool in laboratory tests, through the use of simple control plots. Industrial results validated the ability of the system to differentiate machining data from one day to another, and to isolate an unusual piece of barstock that led to slightly below average part dimensions.

The difficulties experienced in the transitioning from laboratory conditions to industrial testing were discussed. This information will allow future researchers to continue adding new process monitoring sensors to the system.

In conclusion, this research demonstrated the ability of online process monitoring of discrete part manufacturing in a laboratory setting; and brings the MMRI and GMI closer to having a fully implemented process monitoring system for part quality prediction and machine maintenance.

## **Acknowledgements**

Firstly, it is important to acknowledge the support and guidance of Dr. Stephen Veldhuis throughout my career at McMaster University. I value the time at McMaster and all of the experience I have gained.

The learning opportunities and positive experiences I had in the MMRI are largely a result of the support of Terry Wagg. His diligence and patience in helping the students acquire new skills is much appreciated. There is a great team of students in the MMRI who create a strong sense of community and are always willing to help, especially: Andrew Biksa, Jeremy Boyd, Brian Perry, Steven Remilli, and Youseff Ziada. Thank you also to Janet Murphy for assisting in arranging special events for us. Thank you to Maneesh Khanna for always taking the time to present me with feedback and advice on my work. The electrical experience gained in this work was a result of Joe Verhaeghe's guidance.

For his previous work and assistance when requested, I would like to thank Darryl Wallace, at ProSensus. James Nixon at Nixon Integrated Machining Designs Ltd. also provided knowledge and guidance. The assistance on multivariate topics from Kevin Dunn, statistics instructor for the Department of Chemical Engineering, was incredibly appreciated. Additionally, thank you to Emily Nichols for contributing multivariate advice.

Finally, thank you to the entire team at GMI, including Dave Ellison, for making my industrial experience an exciting and excellent learning opportunity.

# Table of Contents

<b>Chapter 1 - Introduction .....</b>	<b>1</b>
1.1 Overview .....	1
1.2 Motivation of Process Monitoring .....	3
1.3 Description of Manufacturing Process Monitoring.....	5
1.4 Thesis Layout .....	7
<b>Chapter 2 - Literature Review .....</b>	<b>9</b>
2.1 Process Inputs.....	9
2.2 Sensing System .....	11
2.2.1 Current Sensor .....	14
2.2.2 Accelerometer .....	17
2.2.3 Thermocouple .....	20
2.3 Signal Processing System.....	22
2.3.1 Data Acquisition .....	22
2.3.2 Data Processing.....	26
2.3.3 Multivariate Statistical Methods .....	32
2.4 Decision Making Strategy .....	46
2.4.1 Hotelling's T2 .....	48
2.4.2 SPE.....	49
2.4.3 Outliers.....	50
2.4.4 Process Control Confidence.....	51
2.5 Process Monitoring Areas of Improvement .....	53
<b>Chapter 3 - Experimental Methods.....</b>	<b>54</b>
3.1 Introduction: Laboratory versus Industrial Testing.....	54
3.2 Instrumentation.....	55
3.2.1 Current Sensor .....	55
3.2.2 Accelerometer .....	57
3.2.3 Thermocouple .....	59
3.3 Data Acquisition.....	61
3.3.1 Sampling Frequency .....	62
3.3.2 Serial Port Trigger.....	64
3.3.3 Data Acquisition Sample .....	66
3.4 Data Processing .....	67
3.5 Multivariate Analysis .....	71

3.5.1	ProMV versus MATLAB .....	71
3.5.2	Model Building: Training & Testing Data.....	73
3.5.3	Model Analysis .....	73
<b>Chapter 4 -</b>	<b>MMRI Laboratory Testing.....</b>	<b>74</b>
4.1	Introduction to MMRI Laboratory Testing .....	74
4.2	Test A – Simulate Disturbances .....	76
4.2.1	PCA Model on All Variables .....	77
4.2.2	2 PCA Models.....	81
4.2.3	PCA Model on Entire Frequency Spectrum .....	82
4.3	Test B – Simulate Changes in Depth of Cut .....	83
4.4	Test C – Simulate Worn Tool .....	87
4.5	PLS Model.....	92
4.6	New Process Data.....	93
4.7	Laboratory Summary.....	96
<b>Chapter 5 -</b>	<b>Industrial Testing .....</b>	<b>100</b>
5.1	Introduction to Industrial Testing.....	100
5.2	Industrial Implementation Challenges.....	101
5.3	Data Acquisition & Analysis.....	103
5.4	Results .....	105
5.5	Industrial Summary .....	111
<b>Chapter 6 -</b>	<b>Conclusions and Recommendations .....</b>	<b>114</b>
6.1	Conclusions .....	114
6.2	Recommendations for Future Work.....	115
<b>Chapter 7 -</b>	<b>Bibliography.....</b>	<b>117</b>
<b>Appendix A.....</b>		<b>121</b>

## List of Figures

Figure 1: Process Monitoring Flow .....	6
Figure 2: Aliasing (Adapted from National Instruments [29]) .....	24
Figure 3: X Data Matrix for Process Monitoring System with Discrete Observations or Batches (Adapted from [34]).....	27
Figure 4: Spindle Current Sensor .....	56
Figure 5: Signal Condition Box for Current Sensors .....	57
Figure 6: Accelerometer mounted on spindle bearing housing of lathe .....	58
Figure 7: Thermocouple Mounting Locations .....	60
Figure 8: Serial Port Communication Cabling Schematic .....	65
Figure 9: Raw Data Sample .....	67
Figure 10: Results of Accelerometer FFT.....	69
Figure 11: Results of Processed Accelerometer FFT .....	70
Figure 12: Spindle with bolt .....	76
Figure 13: ProMV SPE vs. HT2 Plot for Test A .....	78
Figure 14: ProMV Contribution Plot for Observation 3 and 20 from Test Set A	79
Figure 15: ProMV Contribution Plot for Observation 2 from Test A .....	80
Figure 16: ProMV Contribution Plot for Observation 2 from Test Set A – Zoomed to exclude Frequency and Magnitude Information .....	81
Figure 17: ProMV SPE vs. HT2 Plot for Test B.....	84
Figure 18: ProMV Contribution Plot for Observation 6 & 41 from Test B .....	85

Figure 19: ProMV Contribution Plot for Observation 58 from Test B..... 86

Figure 20: ProMV SPE vs. HT2 Plot for Test C..... 88

Figure 21: ProMV Contribution Plot for All Worn Tools from Test C..... 89

Figure 22: ProMV Score Plot for Test C – Components 1 and 2 – Zoomed within  
95% Control Limit ..... 90

Figure 23: ProMV SPE vs. HT2 Plot for Test B with New Process Data ..... 95

Figure 24: ProMV SPE vs. HT2 Plot for Test C with New Process Data ..... 96

Figure 25: GMI Quality Control Chart ..... 104

Figure 26: ProMV SPE vs. HT2 Plot for Industrial Test..... 106

Figure 27: ProMV Loading Bi-Plot for Industrial Test – Components 1 and 2 . 108

Figure 28: ProMV Score Plot for Industrial Test – Components 1 and 2 –  
Zoomed within Day One..... 110

## List of Tables

Table 1: Canadian manufacturing sales for transportation equipment .....	5
Table 2: Objects, Items and Purposes of Sensing .....	12
Table 3: Vibration Sources .....	18
Table 4: Summary of Data Processing Techniques .....	28
Table 5: Accelerometer mounting methods .....	59
Table 6: Data Processing Methods for Sensor Signals .....	71
Table 7: Raw Data, Scores and Loadings for Model Comparison.....	72
Table 8: Test A Observations .....	77
Table 9: Test Set B Observations.....	83
Table 10: Test C Observations.....	87
Table 11: Overview of Observation Clusters.....	91
Table 12: New Process Observations .....	93
Table 13: Industrial Observations .....	105
Table 14: Serial Port Communication FANUC Parameters .....	121

## Nomenclature

AC	Alternating current	LSL	Lower specification limit
ADC	Analog to digital converter	MMRI	McMaster Manufacturing Research Institute
ANN	Artificial neural network	MVA	Multivariate analysis
CMM	Coordinate measuring machine	NIPALS	Non-iterative partial least squares
CNC	Computer numerical control	PCA	Principal component analysis
DAQ	Data acquisition	PLS	Partial least squares
DC	Digital converter	RMS	Root mean square
DFT	Discrete Fourier transform	RPM	Revolutions per minute
FFT	Fast Fourier transform	RS-232	Recommended Standard 232
GMI	Glueckler Metal Incorporated	SPE	Squared prediction error
HT2	Hotelling's T-squared	UCL	Upper control limit
LCL	Lower control limit	USL	Upper specification limit

## List of Symbols

$a$	Denotes $a$ -th principal component
$A$	Total number of principal components
$k$	Denotes $k$ -th variable in data matrix
$K$	Total number of variables in data matrix
$N$	Total number of observations
$p$	Loadings
$Q^2$	Estimate of the predictive ability of the model
$R^2$	Estimate of the variation explained by the model
$t$	Scores
$X$	Refers to data matrix
$X$	Refers to x-axis or x direction
$Y$	Refers to y-axis or y direction
$Z$	Refers to z-axis or z direction

## Chapter 1 - Introduction

### 1.1 Overview

An investigation into the topic of online process monitoring of discrete part manufacturing using multivariate analysis is presented in this thesis. To better understand the thesis title, each of the topics is summarized below.

- **Online process monitoring:** collection of process information in real-time in an automated environment. This topic has been successfully applied in chemical engineering, both academia and industry, particularly in the production of foods and pharmaceuticals.
- **Discrete part manufacturing:** application of process monitoring in the manufacture of individual parts opposed to the continuous nature of many chemical applications. This adds additional complexity to the analysis since each part has natural part-to-part variation, as well as an array of process information collected over a period of time.
- **Multivariate analysis:** statistical technique to analyze and present the process information in a form similar to that of statistical process control. Traditional statistical process control is usually applied to monitor only the quality information and is done offline or at the end of the process. Conversely,

multivariate analysis can be applied to collect information on many of the manufacturing variables and can be completed online. This aids in both troubleshooting applications and in the prediction of part quality.

To validate the application of process monitoring in manufacturing, an experimental setup was completed in the McMaster University Manufacturing Research Institute (MMRI). This setup was then applied in industry at Glueckler Metal Incorporated (GMI). Both setups involved turning of raw barstock on a lathe.

The topic of online process monitoring and multivariate analysis applied to manufacturing is an extension of work completed at McMaster University by Wessam Hussein, B.Sc, M.Sc., Ph.D., Samar Ruparelia, B.Sc., M.Sc., Ph.D., and Darryl Wallace, B.Eng. M.A.Sc. Hussein developed a multivariate classification model of different cutting conditions, including a normal, worn, and chipped tool, as well as chatter, and used another multivariate model to predict surface roughness [1]. Ruparelia was able to relate excited frequency bands produced from an FFT performed on accelerometer data, to the occurrence of drill chipping and created a detailed process flow chart [2]. Wallace had success in compensating for thermal errors, detecting mis-loaded parts, and verifying the production of good quality parts [3]. However, the researchers had difficulties dealing with machining data that contained noise from common process variation and material inconsistencies. The goal of the present research is to extend on the

work by Hussein, Ruparelia and Wallace, to attempt to reduce variability during data acquisition, improve the data analysis process, and implement additional steps that would bring the MMRI closer to having a commercial online process monitoring system installed at a manufacturing facility. Therefore, a lot of this thesis will refer to the research completed by Hussein, Ruparelia and Wallace, as well as others who have made advances in the field of process monitoring.

## **1.2 Motivation of Process Monitoring**

The motivation behind implementing process monitoring is product quality. As stated by Kevin Dunn, a statistics and multivariate instructor: “product quality is not a cost-benefit trade-off”; it is always beneficial for a manufacturer, and its customers, to improve product quality [4]. A manufacturing process with good quality products and low variability will boost profits by lowering costs [4]. Lower costs are a result of minimal scrapped off-specification product and minimal re-work [4]. Furthermore, increased long-term sales follow as a result of loyal customers and improved reputation [4]. However, product quality testing is non-value added. Value creation lies in the manufacturing of high quality products, and utilizing testing methods at reduced rates, to verify the product standards. Thus, rather than waiting until the end of a process to discover a poor quality product, manufacturers should be monitoring, in real-time, the intermediate parts of the process [4]. If unusual variability is discovered, the aim

is to make permanent process adjustments to avoid the variability from ever occurring again [4]. Dunn emphasizes the importance of understanding that process monitoring is not a method of automatic feedback control [4]. These methods do share similarities in terms of quantifying an unusual operation; however, the goal of process monitoring is that the process adjustments are infrequent, usually manual, and take place due to special causes [4]. Therefore, the process variability should already be at a minimum. Process monitoring should be implemented to monitor for unusual process variability that may be a consequence of a disturbance that would result in a poor quality part.

Process monitoring to reduce product variability has the potential to help Canadian manufacturers compete in the global market. A survey performed by KPMG in 2006 predicted a rise in Asian automobiles manufacturers' market share, at the expense of North American manufacturer's market share [5]. Perhaps until the recent Toyota quality incidents of 2010, the North American market had the perception that Asian automobiles are more reliable than North American automobiles [6]. This emphasizes how product variability can drive purchase decisions. In fact, from 2005 to 2009, Canadian manufacturing sales for the transportation and equipment sub sector has declined by over 30%, refer to Table 1 [7]. Although a recent turnaround in perceptions may begin to help the North American automobile market, this will need to be supported by product innovation delivered with improved levels of product quality.

**Table 1: Canadian manufacturing sales for transportation equipment**  
(Adapted from [7])

	2005	2006	2007	2008	2009
Transportation equipment ( <i>\$ millions</i> )	124,740.9	119,387.2	116,597.5	97,446.8	76,063.2

### 1.3 Description of Manufacturing Process Monitoring

The motivations behind utilizing process monitoring as a crucial component in manufacturing process automation are evident. The major elements of a manufacturing process monitoring system, adapted from Hussein [1] are:

1. Manufacturing process inputs including the operating parameters such as feed rate, depth of cut and cutting speed.
2. Sensing system to detect changes in the process conditions, through measurement of various process features.
3. Signal processing system, including both a means of pre-processing the data, and then analyzing that information.
4. Decision making strategy, which should be based on an established confidence level.

The schematic, shown in Figure 1, summarizes the flow of data in process monitoring, and relates well to the concepts that will be discussed in the following sections. Process monitoring follows a continuous cycle in which product quality is the driving force.

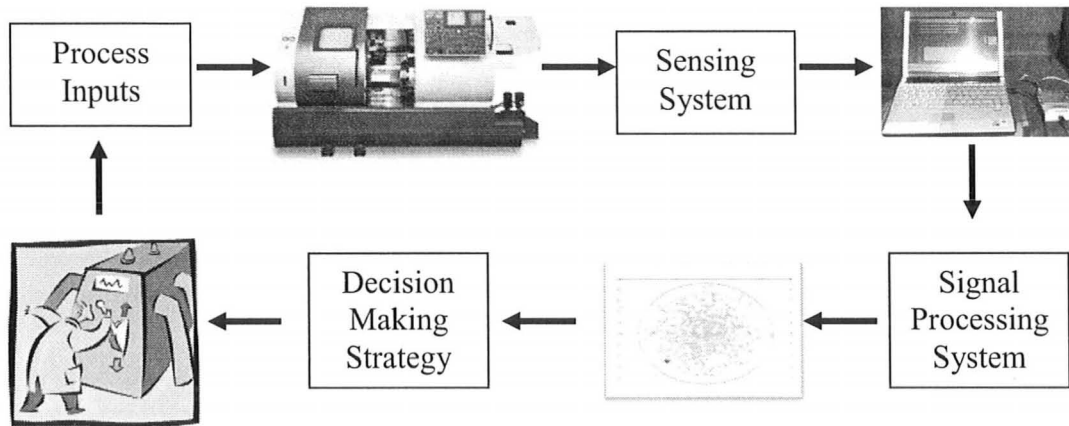


**Figure 1: Process Monitoring Flow**

Implementing process monitoring in a manufacturing setting does present some unique challenges. Firstly, production rates are commonly high so there is not a lot of downtime available to install and maintain the system. Therefore, the necessary instrumentation must be applied in an effective and economical way with minimal to no effect on production. This involves the use of indirect sensors which are applied outside of the cutting zone. Also instrument selection is important, since the process data commonly has a low signal to noise ratio. High production rates also mean high data volumes, so data compression and storage becomes important. Additionally, the process data commonly has correlations that are difficult to determine univariately, as well as missing data due to many factors that occur within the machining environment. Thus, statistical techniques are required to handle the process data in an efficient and meaningful way. The

overall result needs to be an autonomous online process monitoring system that will alert an operator of a control issue only when necessary. The individual elements, as outlined by boxes in Figure 1, will be considered in Chapter 2.

## **1.4 Thesis Layout**

This thesis will begin with a literature review that is structured around the process monitoring flow chart shown in Figure 1. The literature review presents a detailed summary on each of the flow chart topics: process inputs, sensing system, signal processing system and decision making strategy. Although considerable time was taken to understand all the background information, the goal was to build upon the work completed by Hussein, Ruparelia and Wallace. Therefore, the literature review discusses general process monitoring topics, and then focuses on the relevant sensors and analysis techniques as recommended by the previous researchers.

Following the literature review, the experimental methods are discussed as they apply to both laboratory and industrial testing. The experimental methods follow in a similar order as the literature review, with a discussion of how the sensors were instrumented, detailed data acquisition techniques, and finally multivariate analysis.

The laboratory and industrial testing details and results are presented in subsequent chapters. Each of these chapters finishes with a summary and

recommendations for future research. The thesis finishes with the concluding statements.

## **Chapter 2 - Literature Review**

### **2.1 Process Inputs**

Successful process monitoring begins with a meticulous understanding of the process to be examined. Figure 1 outlines the first important step in process monitoring: a consideration of all the process inputs. Process inputs refer to all the internal, external, both desired and undesired, features relating to the system.

Internal features are those that have to do specifically with the process, and are usually entered by an operator; these features may include the desired setting for feed rate, constant surface speed, depth of cut, use of coolant, bar stock material, and insert selection. For example, it is common to hold machining parameters constant; however, Hussein selected a range of machining parameters based on the capability of each of the three machines he performed testing on [1]. A series of spindle speeds, depth of cut, and feed per tooth was selected [1]. Each of these selections was included in the process monitoring model to ensure no unintended effect on the results [1].

External features are those that affect the system, but are not set by the operator, such as room temperature and humidity levels. Undesired features are those that may cause variances in the process, such as random floor vibrations

from other machines, and hard particles in the barstock material. The goal in process monitoring is to detect these undesired features since they have the potential to adversely affect product quality.

When building a successful process monitoring model one must consider the fundamentals of design of experiment techniques. Properly designed experiments require a realization of all the confounding effects. Confounding effects are disturbances in the experiment that will likely alter the experiment and result in difficulty when analyzing the outcomes. Therefore, it is important to take time to carefully understand the process and all of the confounding effects. Disturbances that are known, controllable, or measurable should either be eliminated if possible, or recorded and included into the model. An example of a known confounding effect that should be included in a process monitoring model is raw barstock length in a turning application [8]. As the barstock becomes shorter, its natural frequency will change, resulting in a change in the vibration spectrum. If this change is not included, the vibration data will vary, making it difficult for the model to predict any meaningful information. Therefore, understanding all the process inputs allows for the unknown confounding effects that may affect product quality to be detected more readily.

## 2.2 Sensing System

Following the flow chart from Figure 1, the next important feature is the sensing system. A suitable sensor system is imperative to the application of process monitoring. The topic of sensor fusion, which is the combination of multiple sensors, increases the reliability of a sensing system [9]. The use of sensor fusion makes the process monitoring system redundant so that various types of malfunctions that occur in the process can be detected, while also reducing the chance of incorrect analysis from inherent randomness or noise, and sensor drift [9]. Sensor selection depends on the objects to be sensed and the purpose of monitoring, as outlined in Table 2 [9]. Sensor selection is a difficult task because sensors depend on the following characteristics: ambient operating temperatures, full-scale output, hysteresis, linearity, measuring range, operating life, output format, overload, repeatability, resolution, selectivity, sensitivity, response speed, and stability or drift [9].

**Table 2: Objects, Items and Purposes of Sensing  
(Adapted from [9])**

<b>Object of sensing and monitoring</b>	<b>Items to be sensed</b>	<b>Purpose of sensing and monitoring</b>
Work	State of work clamping Geometrical and dimensional accuracy Surface roughness Surface quality	Maintain high quality Avoid damage and loss of work
Machining process	Force Heat generated Temperature Vibration Noise and sound Chip formation process	Maintain normal machining process Predict and avoid abnormal state
Tool	Tool edge position Wear Damage: chipping, breakage, and others	Manage tool changing time Avoid damage or deterioration of work
Machine tool and auxiliary facility	Malfunction Vibration Deformation (elastic, thermal)	Maintain normal condition of machine tool and ensure high accuracy
Environment	Ambient temperature change External vibration Condition of cutting fluid	Minimize environmental effect

After in-depth review of possible sensors by Hussein, the following were selected: a table dynamometer to measure  $X$ ,  $Y$  and  $Z$  axis forces, accelerometer to measure spindle bearing vibration, acoustic emission sensor, and a current sensor to measure spindle motor current [1].

Dynamometers are commonly used in the laboratory environment [10]. The MMRI frequently uses a dynamometer in tool wear and coating tests. Although dynamometers are popular in academia, there are many issues that make them difficult for industrial implementation [10,11]. Firstly, dynamometers have a high price point, making it difficult to purchase one for each machine in a

manufacturing plant. Secondly, they can be heavy and awkward to apply to a machine, increasing the downtime required for installation. Thirdly, they need to be mounted within the cutting zone, leading to a possible disruption in machining if there are sensor problems, as well as a shortened life due to the harsh conditions including chips and coolant. Instead cutting force has been measured by use of motor current [10,11,12].

Acoustic emission sensors have shown the ability to predict events such as sudden crack formation and propagation as well as chip breakage [13]. However, Hussein concluded that the acoustic emission sensors showed poor performance and was not suitable for his application [1]. Furthermore, to detect such events as crack propagation, sampling rates on the order of megahertz are required. These high sampling rates demand a lot of the data acquisition bandwidth, computer analysis, and storage systems, making the acoustic emission sensor impractical for industrial use.

Since Ruparelia's focus was on drill chipping, he ruled out the dynamometer because Li et al. showed that it is more suitable for detecting drill wear not chipping [2,14]. Ruparelia examined the acoustic emission sensor and suggested that benefits of using this device include: placement next to drilling location is not crucial since the acoustic emission signal propagates through the entire workpiece; and the acoustic emission frequency is usually much higher than the natural frequency of the drilling process, meaning it cannot be misinterpreted

for vibration during normal drilling [2]. However, he chose not to use the acoustic emission sensor due to its high cost. Ruparelia chose to use a low cost accelerometer [2].

Wallace's sensor selection was more tailored for an industrial based process monitoring system, than Hussein's, as he selected sensors capable of measuring critical machine process conditions without interfering or being interfered with the machining process [3]. However, as the sensors become more removed from the cutting zone, the signal to noise ratio will decrease. This research will follow Wallace's sensor selection by focusing on motor current sensors, an accelerometer, and thermocouples.

### **2.2.1 Current Sensor**

Measurement of motor current has been shown to be an acceptable method of collecting process information when more direct techniques are difficult or not possible [3,11,10,12]. Wallace presented a method by Jeong and Cho (2002) of using feed motor currents on a milling machine for an estimation of cutting forces [3,15]. Wallace also presented work by Li et al. in 2003, in which Hall-effect current sensors were used to monitor spindle current for the diagnosis of a tapping process; with a 93% success rate in differentiating between five different process conditions [3,16]. In 2005, Li used Hall-effect current sensors to measure the cutting forces in turning [11]. He stated that other researchers have accurately

measured cutting forces with various Kistler apparatus's, but these are expensive, and have limitations including sensor reliability in the harsh environment, layout constraints, and interference with cutting performance [11]. Li suggests that measuring motor current is a good method of overcoming these disadvantages [11]. Li emphasized the benefit of current sensors because they are a simple and inexpensive method of modelling tangential, axial, and radial cutting forces in turning [11]. Li compared estimated cutting forces calculated from models based on current sensor data, to actual cutting forces collected by a Kistler cutting force dynamometer [11]. The estimated and actual cutting forces showed good agreement, with the difference between measured and estimated cutting forces less than: 10 % for tangential, 5% for axial, and 25% for radial [11].

Cutting force estimation, such as that done by Li, is important since cutting force is dependent on the material cut, chip geometry, tool configurations and cutting speed. A change in cutting force can indicate events such as chatter or chatter marks left behind from a previous pass, chip tangling, numerical or operator errors, and collisions. Measured cutting forces can be resolved into three components: cutting direction, feed direction and normal to cutting direction [9]. Analysis of the cutting and feed force directions can indicate surface finish or the presence of tool chipping or breakage [9]. The normal to cutting direction can indicate the dimensions of the feature being machined [9]. However, as Li showed, estimating the actual forces based on the indirect measurement by a

current sensor can be prone to some error. Jeong and Cho also concluded that the estimates of the cutting force normal to machined surface included some error, due to factors such as stick-slip friction, and could be improved by using well-machined feed drive parts [15]. Fortunately, using current sensors in process monitoring does not require an estimation of the force, but rather a repeatable and reliable measure of the change in current from one part to another as a representation of features such as tool wear, surface finish, and part dimensions.

Wallace employed current sensors fixed to motor power leads in the electrical panel of the machine [3]. In terms of specifics, Wallace's research utilized the following current sensors: open loop Hall-effect current sensor from F.W. Bell, model IHA-150 for the Z motor, and a clamp type style current sensor for the spindle motor [3]. Hussein used the same open loop hall-effect sensor from F.W. Bell, but applied it to the spindle motor [1].

When discussing the types of current sensors used by Hussein and Wallace, two characteristics should be considered: Hall-effect, and open loop versus closed loop. The Hall-effect was discovered by Dr. Edwin Hall in 1879 [17]. Dr. Hall found when a magnet was placed so that its field was perpendicular to one face of a thin rectangle of gold through which current was flowing, a difference in potential appeared at the opposite edges [17]. He found that this voltage was proportional to the current flowing through the conductor, and the flux density or magnetic induction perpendicular to the conductor [17]. Hall-

effect sensors can be applied to sensing devices when the object to be sensed incorporates a magnetic field [17]. When current flows through a conductor, it creates a magnetic field around the conductor [17]. This magnetic field is in direct proportion to the current level [17]. If the drive current is controlled using a constant current source and the differential Hall voltage is amplified, an output voltage proportional to the primary current can be obtained by the electronics in the circuit [17]. This core Hall-effect sensor, referred to as an open-loop sensor requires power to operate, but much less than that of a closed-loop sensor. It also has a higher ability to withstand overloads. When cost is a major consideration, a basic open loop sensor should be selected. Closed loop on the other hand, is less susceptible to electrical noise and should be selected based on its fast response, accuracy, and linearity better than 0.1% [17]. However, the closed loop sensors are more expensive due to the addition of several more components including an operational amplifier and coil [17].

### **2.2.2 Accelerometer**

Accelerometers are widely used in industry as a means of monitoring and collecting vibration information. Vibration measurements are important because depending on the cutting conditions and dynamic properties of the system, machine tool errors can arise as a result of a cutting operation. Machine tool errors directly affect part quality and surface finish. Vibrations that occur during

cutting can be classified as free or forced. Free vibration occurs when the system is left to vibrate on its own after an initial disturbance [18]. Forced vibration occurs when a system is subjected to an external force, which is often repeating [18]. Forced vibration can be divided into the following categories: external forces, forces independent of the cutting process, and forces initiated by the cutting process. Ruparelia outlined the different vibrations sources, as shown in Table 3 [2]. The goal of using an accelerometer in manufacturing process monitoring is to detect any or all of the sources of vibration that have potential to affect part quality.

**Table 3: Vibration Sources  
(Adapted from [2])**

Free	Forced		
<ul style="list-style-type: none"> <li>• Sudden shock caused by material inhomogeneities</li> <li>• Chipping</li> </ul>	External	Independent of Cutting Process	Initiated by Cutting Process
	<ul style="list-style-type: none"> <li>• Generated by nearby machines or factory floor</li> </ul>	<ul style="list-style-type: none"> <li>• Disturbance in workpiece or tool drive system</li> </ul>	<ul style="list-style-type: none"> <li>• Fluctuating forces during cutting</li> <li>• Removal of chips</li> </ul>

An accelerometer is built using a tuned mass, that when displaced by a vibration, generates a charge across a piezoelectric crystal. The piezoelectric effect was discovered in 1880 by Pierre and Jacques Currie [19]. The piezoelectric effect describes how a piezoelectric material produces an electric charge in response to a mechanical stress [19]. Commercial piezoelectric materials, such as those in an accelerometer or dynamometer, are achieved by

exposing the materials to high temperatures while imposing high electric field intensity in the desired direction [19].

Inasaki and Tonshoff discussed in *Sensors and Manufacturing* (2001) that accelerometers can easily be applied to a machine tool component and do not need to be mounted close to the zone of contact because the frequency detected does not suffer severe distortion [9]. Risbood et al. used an accelerometer for surface roughness prediction in a cylindrical turning operation [20]. Ruparelia presented work by El-Wardany et al. which involved using an accelerometer to detect drill failure for small diameter drills [2,21]. El-Wardany et al. and Ruparelia's work used processing techniques such as kurtosis for the vibration data in time domain, and cepstrum ratio for in the vibration data in frequency domain, and did not utilize multivariate analysis [2,21].

Ruparelia used only one Kistler accelerometer 8702B25 mounted in the transverse direction to the center of the fixture securing the workpiece [2]. He connected the accelerometer to a charge amplifier, Kistler 8004, and a four channel data acquisition board and computer [2]. Ruparelia performed drilling, while periodically examining the cutting edge using a tool maker's microscope, until chipping occurred [2]. At the first sign of chipping, analysis of time-domain vibration signal belonging to the drill was detected in order to identify the signature of chipping [2]. In the time domain, small vibration spikes appeared randomly, likely due to material inconsistencies or chip accumulation and not drill

chipping [2]. However, in the frequency domain, excited frequency bands could be identified that corresponded with drill chipping [2].

Wallace used three Kistler accelerometers, 8702B50, mounted within the spindle structure behind the covering panel of the machine, at a safe location outside of the cutting zone [3]. Wallace mounted the accelerometers on a one inch cube with tapped holes [3]. Hussein used the same Kistler accelerometer clamped on the spindle motor by means of a magnetic clamp [1].

### **2.2.3 Thermocouple**

Temperature measurements are important because temperature accounts for approximately 70% of the total error in machine tools [22]. Thermal sources include: room temperature, use of coolant, exposure to sunlight, motors, bearings and ball screws [22]. Wallace introduced research completed by Veldhuis on the geometric deformation of machine tools as a result of thermal effects [3,23]. Veldhuis outlined the thermal errors affecting a machine initially at room temperature in the following order: local heating at spindle motor and spindle bearing, spindle support heats up, ballscrews and gears heat up, local heating in Z column, and entire Z column heats up [23]. Veldhuis indicated that the listed thermal errors can cause extreme deformation in the machine [23].

All researchers mentioned above utilized thermocouples in their work. A thermocouple is the most widely used temperature measurement device due to its

simplicity, ability to measure over a wide range, and low cost. The underlying physics that describes the function of a thermocouple is the Seebeck, or thermoelectric effect. This effect occurs when two dissimilar metals joined together at one end, referred to as the hot junction, are heated or cooled, produce a voltage that can be correlated back to the temperature [24]. The other end of the wires must always be connected to a cold junction [24]. The voltage is dependent on the difference in temperature between the hot and cold junction, and the material of each of the wires [24]. Each material combination is suitable for a different temperature range and environment [24]. Omega recommends selecting a thermocouple based on: temperature range, chemical resistance, abrasion and vibration resistance, and installation requirements [24].

Wallace utilized E-type thermocouples [3]. E-type thermocouples have a temperature range of approximately  $-200^{\circ}\text{C}$  to  $900^{\circ}\text{C}$ , and greater than  $1.7^{\circ}\text{C}$  standard limits of error [24]. Wallace mounted the thermocouples on the following locations of a CNC milling machine: ambient, front spindle, spindle chiller, spindle motor base, spindle housing structure to measure Z column, motor bases to measure X, Z and Y [3].

Yang et al. used thermal error mode analysis to reduce the number of thermal sensors used on a CNC turning center from 16 to four, and to reduce the thermal error [25]. Although thermistors were used instead of thermocouples, this research is particularly relevant since it was applied to a turning center. Thermal

sensor placement on the turning center included the following locations: spindle housing, ball screw bearings and nuts, coolant tanks, and machine structure [25].

## **2.3 Signal Processing System**

From Figure 1, the next important feature is the signal processing system. However, this feature encompasses many steps within the process monitoring system. Therefore, it has been divided into three sections in order of usage in a process monitoring application: data acquisition, data processing, multivariate analysis.

### **2.3.1 Data Acquisition**

In order to acquire signals from the various sensors, the sensors must be connected to a data acquisition (DAQ) system. Data acquisition is the process of retrieving data from sensors and inputting that data into a computer for processing [26]. A DAQ board is a printed circuit board that provides amplification and analogue-to-digital conversion (ADC) [26]. ADC is important because output from most sensors, including accelerometers, tends to be in analogue form. A DAQ card has a clock that supplies regular time signal pulses to its analogue to digital converter, and every time it receives a pulse, it samples the analogue signal [26]. Selecting an appropriate sampling rate for data acquisition is a very important task.

A sampling frequency is usually selected based on a known frequency of interest. However, if the frequency of interest includes the region of rpm, as well as unknown frequencies, sample rate,  $f_s$ , selection is not straightforward. Knowing that sensor data is commonly analyzed using spectral analysis the following tips were considered from Lyons text on Discrete Signal Processing [27]. The application of spectral analysis and fast Fourier transforms (FFT) will be discussed in 2.3.2.

1. Sample at 2.5 to 4 times the signal bandwidth [27].

Sampling at least 2.5 times higher than the signal bandwidth aids in avoiding aliasing. An aliased signal provides a poor representation of the analog signal, by allowing a false lower frequency component to appear in the sampled data of a signal, illustrated in Figure 2 [28]. This figure illustrates that as more samples are collected within the same period of time, a higher frequency signal appears.

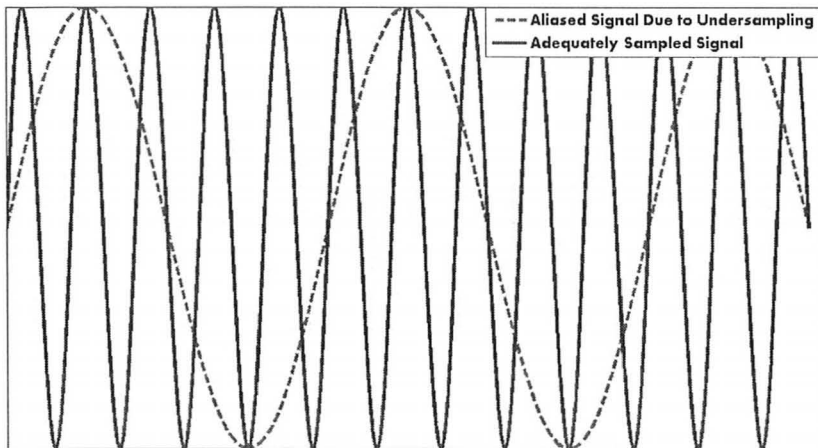


**Figure 2: Aliasing (Adapted from National Instruments [29])**

The maximum frequency that can be accurately represented without aliasing is the Nyquist frequency [28]. The Nyquist frequency is equal to one-half of the sampling frequency [28]. Therefore, to prevent aliasing by following the Nyquist theory, the sampling frequency should be at minimum two times higher than the frequency of interest, assuming that frequency is known. National Instruments recommends sampling even higher, at ten times the signal bandwidth [28].

## 2. Increase frequency resolution [27].

A high frequency resolution is important to avoid spectral leakage. Spectral leakage occurs when a data signal has frequency components in between the frequency bins, causing the signal to show up to some degree in all of the output frequency bins [27]. The relevant frequencies produced by the FFT are given by the following range:  $[0, f_s/2]$ . The frequency spacing is referred to as the bin spacing, and is given by equation (1), where  $N$  is the number of samples [27].

$$\text{bin spacing} = \frac{f_s}{N} \quad (1)$$

To increase the frequency resolution, in other words, decrease the bin spacing, for a given frequency range, one should increase the number of samples collected at the same sampling frequency [29]. As shown in equation (2), this can only be done by increasing the sampling time. Changing the sampling frequency will not affect the frequency resolution, since as the sampling frequency changes, so does the number of samples collected.

$$\text{bin spacing} = \frac{f_s}{N} = \frac{f_s}{f_s \times t} = \frac{1}{t} \quad (2)$$

## 3. Consider frequency of interest [27].

Another method of preventing spectral leakage is to choose a sampling frequency and sampling time such that the frequency of interest, if known, will lie exactly on a bin center [27]. For example, given an integer frequency of interest,

sampling at any sampling frequency for one second, will force a bin center of one, ensuring no spectral leakage.

4. Number of samples should be equal to a power of two [27].

Ensuring that the number of data samples collected during data acquisition is a power of two results in faster FFT calculations. This can be done by appropriate selection of the sampling frequency and time period or by zero padding. More details about zero-padding will be discussed in 2.3.2.

Hussein sampled all data at 33 kHz [1]. Ruparelia sampled at 24,242 Hz, which corresponded to 1500 data points per revolution [2]. Wallace initially sampled at 10 kHz, but found that 2 kHz was acceptable [3].

### **2.3.2 Data Processing**

One of the difficulties with manufacturing process monitoring is that each observation is actually a discrete part with many sensor signals associated with it, and each sensor signal has an array of time domain data. Conversely, a chemical process monitoring system may monitor a continuous flow of liquid with sensor signals acquired at specific intervals. In this case, each observation represents a single point in time. A manufacturing process monitoring system is analogous to chemical batch processes. Batch data is difficult to analyze since the data matrix, denoted by  $X$ , is essentially three-dimensional, as shown in Figure 3.

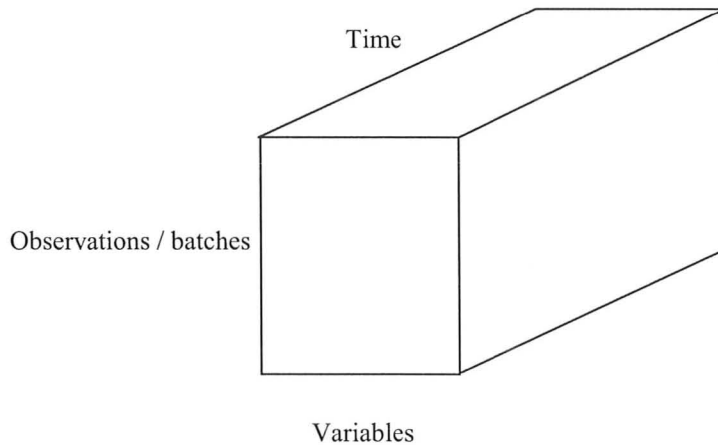


**Figure 3: X Data Matrix for Process Monitoring System with Discrete Observations or Batches (Adapted from [34])**

One of the simplest methods to analyze this type of data is to process it by means of averaging. For example, data acquired at 10 kHz, for one second, results in 10,000 data points; taking an average over the entire time domain signal results in a compression of the 10,000 data points into a single value. Of course, compression always results in some loss of information. Therefore, the goal is to carefully select the type of data processing method that will limit the loss of relevant information.

Table 4 shows a summary of the data processing techniques used by Hussein, Ruparelia and Wallace for each of the sensors.

**Table 4: Summary of Data Processing Techniques  
(Adapted from [1,2,3])**

	AE	Current	Force: x, y	Temperature	Vibration
<b>Hussein</b>	Mean	Mean	<ul style="list-style-type: none"> <li>• Mean</li> <li>• FFT – maximum of 2 kHz frequency band</li> <li>• Resultant force rations: <math>F_{rx}, F_{ry}</math></li> </ul>	-	Mean
<b>Ruparelia</b>	-	-	-	-	<ul style="list-style-type: none"> <li>• Time domain</li> <li>• Frequency domain</li> <li>• Wavelet</li> </ul>
<b>Wallace</b>	-	Mean	-	Mean	<ul style="list-style-type: none"> <li>• Magnitude of FFT at tooth passing frequency</li> </ul>

Both Hussein and Wallace used a mean calculation for many of the sensors [1,3]. In the case of sinusoidal data, root mean square (RMS) is more applicable than mean. The RMS is given by equation (3).

$$RMS = \sqrt{\frac{\sum_{i=1}^N x_i^2}{N}} \quad (3)$$

Spectral analysis was applied by Hussein, Ruparelia and Wallace in order to break down the time domain sensor signals into their main components as represented in the frequency domain [1,2,3]. Spectral analysis is commonly used

when analyzing data from dynamometers, accelerometers, and acoustic emission sensors, in order to find the frequency components of the signal within the time domain signal. The discrete Fourier transform (DFT) can be used to transform an expression of a continuous time domain function into a continuous frequency domain function [27]. The concept behind the DFT is that any output signal is nothing more than the sum of term-by-term products of cosine and sine waves [27]. Using the DFT, it is possible to determine the frequencies that correspond to the signal, allowing for a more effective interpretation of the signal. Equation (4) is the expression used to transform a continuous time domain function  $x(t)$  into a continuous frequency domain function  $x(f)$ ; where  $j$  is the imaginary unit,  $f$  represents hertz, and  $t$  represents time [27].

$$x(f) = \int_{-\infty}^{\infty} x(t) e^{-j2\pi ft} dt \quad (4)$$

In statistical signal processing, the FFT is the most commonly used method of spectral analysis, since it has the same characteristics and accuracy as the DFT, but is much more efficient [27]. Computational software such as MATLAB has a built in function for FFT calculations. MATLAB uses the following FFT algorithm to return the DFT to the user, as adapted in equation (5); where  $\omega_N$  refers to the  $N$ th root of unity given by equation (6) [30].

$$X(f) = \sum_{j=1}^N x(t) \omega_N^{(t-1)(f-1)} \quad (5)$$

$$\omega_N = e^{(2\pi i)/N} \quad (6)$$

Although MATLAB performs the FFT, it is important to have an understanding of the appropriate application of the FFT in data acquisition. The guidelines listed in 2.3.1 regarding sample rate selection aid in collecting data that will produce the most accurate representation of the data in the frequency domain. The guidelines listed below can be applied after data collection to further improve the frequency domain results.

1. Number of samples should be equal to a power of two [27].

When the situation does not allow for sampling at powers of two, zero padding can be applied to add additional samples to the original input to increase the total number of data samples [27]. However, there is some debate as to the importance of this guideline. Recent information suggests that the importance of the power of two may be decreasing with improved computer processors. Additionally, National Instruments posted information suggesting that zero padding has a high perceived value relating to improving the speed and resolution of the results; but, it can actually lead to results that are easy to misinterpret [31]. For example, if the frequency of interest was known, and bin selection techniques were carried out, zero padding will actually cause a shift in the frequency spacing. In some cases, the fact that the bin center is no longer on the frequency of interest may outweigh the benefit of any efficiency gain [31]. The shift in the bin center, from decreased frequency spacing, corresponds to a resolution increase; however,

this does not improve the frequency resolution of one's analysis of the input signal, since the original sampling frequency did not change [31]. Therefore, it is important to remember to take caution when applying zero padding, and remember that zero padding does not improve signal resolution; this can only be done by increasing the time duration, as discussed previously. MATLAB does not automatically zero pad, but this option is available in the MATLAB FFT function.

## 2. Average multiple FFT's [27].

In the event that there is enough time domain data available, averaging multiple FFT's can improve the sensitivity of the FFT analysis; this allows for detection of the signal energy in the presence of noise [27], which is common in most data acquisition applications.

## 3. Use windowing techniques [27].

A window is a mathematical function applied to the signal to minimize side lobes produced by spectral leakage [27]. There are various types of windows that can be applied, each depending on their specific application, such as: rectangular, triangular, Hanning, and Hamming [27]. Appropriate window selection can be confusing, so National Instruments suggests using a Hanning window for general-purpose applications, spectral analysis, and unknown content [32]. If zero padding is necessary, ensure that the window is applied to the data prior to zero padding [27].

### 2.3.3 Multivariate Statistical Methods

After data acquisition and processing is complete, multivariate statistical methods can be used to analyze the data. Multivariate methods are required to treat process data which commonly have the following characteristics, as outlined by ProSensus [33]:

1. High dimensional data matrices - many observations and many variables
2. Non-causal in nature – cannot imply cause and effect relationships, but can gather information on the correlation relationships
3. Variables are not independent – high correlation among variables
4. Missing data – 10 to 20 % common in industry – or different sampling frequencies among the variables
5. Low signal to noise ratio – each variable contains little information

Traditional data analysis, such as multiple linear regression and statistical process control, is not suited for monitoring a manufacturing process because these techniques require a small number of independent variables and a small number of response variables, usually one [33]. Therefore, large multivariate data sets, such as the ones acquired during manufacturing process monitoring require multivariate statistical techniques.

Characteristic 3– variables are not independent – is particularly important. Standard design of experiment techniques ensure that all factors are independent of one another, allowing the data to be modelled by multiple liner regression,

since the data matrix is of full rank. A full rank matrix is one in which all vectors in the matrix are linearly independent. However, recall that in manufacturing process monitoring the concept of sensor fusion is applied, and involves using multiple sensors to establish redundancy. Redundancy implies that some sensors will be collecting data that is correlated with another sensor. Multiple linear regression fails in the case of highly correlated data because the determinant of the matrix approaches zero and the regression coefficients become inflated. However, with the use of latent variables, multivariate analysis easily handles the correlation resulting from sensor fusion and the nature of the manufacturing process.

There are other methods of analysis that have been used in academia, such as artificial neural networks (ANNs). Both Hussein and Wallace investigated ANNs and other analysis methods, and concluded that multivariate analysis is preferred [1,3]. Hussein summarized some of the problems associated with using ANNs: uncertainty concerning the training time length required, risk of over fitting the data, the overall black-box nature of the method, and an inability to probe the data for root cause analysis [1]. Hussein concluded that all of these issues are of significant importance when considering industrial applications [1]. Hussein also concluded that although multivariate analysis is the preferred solution for manufacturing process monitoring, all the reported works focused on batch and continuous process monitoring applications such as reactors, distillation

columns, fermentation, steel making, and natural gas pipelines; while there was no reported work on machining processes [1].

Multivariate analysis can be divided into two main techniques depending on the data set and the goal of the analysis: principal component analysis (PCA), and projection to latent structures (PLS). Both techniques seek out the latent, in other words hidden, variables in the data.

### **2.3.3.1 Latent Variables**

Dunn presented a simple conceptual example of a latent variable – one's health [4]. Although overall health is extremely important, there is no single measurement to represent health [4]. Instead it is an abstract concept that doctors infer by use of blood pressure values, cholesterol level, weight, and many other measurements [4]. Therefore, health is a latent variable that can be defined by other measurements which all contribute to an assessment of overall health. Another conceptual example of latent variables was given by ProSensus. ProSensus suggested that a television is an example of a latent variable; a television is a two-dimensional representation of the three-dimensional world [33]. This means that a television uses two latent variables to represent what are three dimensions in the real-world [33].

The significance of latent variables is that they compress a large number of variables collected on a subject into a smaller, easier to interpret number of

variables. Latent variables are created by using modelling techniques that find correlations between the original variables. This thesis will show that in machining for example, vibration, current and temperature can be measured to represent an overall product quality. As discussed previously, these sensors are likely not independent. The modelling techniques group together the correlated data, creating a set of latent variables which are independent and best summarize product quality. As defined by Dunn, latent variables have the following characteristics [4]:

1. Latent variables capture an underlying phenomenon in the system being investigated
2. Actual measurements taken on the system are correlated with the latent variable
3. Latent variables are independent or orthogonal to each other

In the case of a principal component model, such as PCA or PLS, the latent variable model objectives are to orientate the latent variables in the direction that gives the greatest variance to a matrix of scores. In summary, a principal component model breaks down the raw data into two parts [4]:

1. A latent variable model, given by:
  - a. Scores ( $t$ ) – distance from origin of  $X$  to a 90 degree projection of each observation onto a line of best fit describing the  $X$  data
  - b. Loadings ( $p$ ) – a direction vector that describes the line of best fit
2. A residual error describing how the model relates to the original data – given by the perpendicular distance from each point in  $X$  onto the plane created by the latent variables

### 2.3.3.2 Principal Component Analysis

Principal Component Analysis (PCA) is used for the single data matrix  $X$ , to find the latent variables and the residual error. The goal of PCA is to find the latent variables that explain the greatest possible amount of variation in  $X$ . From Figure 3,  $X$  has  $N$  rows, where each row represents a different observation, and  $K$  columns, where each column represents a different variable. The time domain data has already been compressed using data processing techniques from 2.3.2. In machining, each row may represent a newly machined part, and the columns may represent data collected from the various sensors. It is common for the  $X$  matrix to have very large  $N$  and  $K$ , or small  $N$  and very large  $K$ . For more than three  $K$  variables it would be difficult to analyze this type of data univariately. Scatter-plot matrices can be used to visualize the correlation between the many variables, but this can be difficult as the number of variables increase.

The PCA model can be calculated using eigenvalue or singular value decomposition, or the non-linear iterative partial least squares (NIPALS) algorithm. The NIPALS algorithm is used by most computer software packages, so the focus will only be on this method. The benefit to using NIPALS is the ability to handle missing data and calculation of the components sequentially. NIPALS calculates the scores ( $t$ ) and loadings ( $p$ ) that are used to describe the model. The algorithm to calculate each of the principal components, denoted by  $a$ , is as follows [4]:

1. Data pre-processing of raw  $X$  matrix
  - a. Mean-center by subtracting each column by its mean: moves the data to the center of the coordinate system to remove any arbitrary bias used when taking measurements
  - b. Scale the data to unit-variance by dividing each column by its standard deviation: removes the fact that the variables are in different units of measurement

Result: each variable in  $X$  is centered in the coordinate system and has equal scaling. Recall that  $X$  has dimensions  $N$  by  $K$ .

2. Create an initial column of scores ( $t$ ) with  $N$  rows - any of the following methods can be used as long as  $t$  is not a column of zeros:
  - a. Generate set of random numbers
  - b. Arbitrarily select a column of  $X$

c. Select column of  $X$  with the maximum variance

3. Take every column in  $X$ , and regress it onto this initial column  $t$ , and store the regression coefficients as the loadings ( $p$ ). This step is analogous to ordinary least squares regression, shown in equation (7), in which the  $y$  variable is replaced with columns of  $X$ .

$$y = \beta x \rightarrow x_k = p_{k,a} t_a \quad (7)$$

Using the ordinary least squares regression equation, and considering the entire  $X$  matrix, the loadings can be calculated by equation (8). Transposing  $p$  is important because it is commonly expressed in terms of  $K$  rows.

$$p_a^T = \frac{1}{t_a^T t_a} t_a^T X \quad (8)$$

4. The loading vector  $p$  has both magnitude and direction. It must be rescaled to have a magnitude of exactly one, making it a unit-vector.

$$p_a^T = \frac{1}{\sqrt{p_a^T p_a}} p_a^T \quad (9)$$

5. Regress every row in  $X$  onto the normalized loading vector. The  $y$  variable this time is replaced with rows of  $X$ , equation (10).

$$y = \beta x \rightarrow x_i = t_{i,a} p_a \quad (10)$$

The regression coefficient becomes the score ( $t$ ) values for each row.

$$t_a = \frac{1}{p_a^T p_a} X^T p_a \quad (11)$$

6. Iterate steps 3 to 5 until the change in vector  $t$  from one iteration to the next is small, usually  $10e-6$  or  $10e-9$ .
7. On convergence, the final score and loading vectors,  $t$  and  $p$ , are stored in the  $a$ -th column in the matrix  $T$  and  $P$ , respectively. These values represent the latent variable of principal component  $a$ . A principle component has the following characteristics:
  - a. It is a line in  $X$  that best approximates the data
  - b. The line explains the greatest possible amount of variation
  - c. The line goes through the average point
  - d. The direction of the line is determined by the loading vector,  $p_a$
  - e. The position of each point,  $i$ , on the line is  $t_{ai}$  [33]
8. Deflate the  $X$  matrix to remove the variability captured by the modelled component.

$$E_a = X_a - t_a p_a^T \quad (12)$$

$$X_{a+1} = E_a \quad (13)$$

For the first component,  $X$  is simply the pre-processed data. For the following components,  $X$  is actually the residual after the previous components were calculated. Deflating the  $X$  matrix ensures that each new component is only seeing the variation remaining, guaranteeing that each component is orthogonal and that no two components can explain the same type of variability.

9. Go back to step 2 and repeat the entire process for the next component until a satisfactory amount of variation has been modelled, without over-fitting the data.

The amount of variation explained by the model is represented by the value  $R^2$ . Equation (14) refers to the overall  $R^2$  value of a model with a total of  $A$  components [4].

$$R_A^2 = 1 - \frac{Var(E_A)}{Var(X)} \quad (14)$$

Cross validation can be used to avoid over-fitting. As successive components are added, the variation in the model is better explained, and the value of  $R^2$  will increase. However, at a certain point, additional components will begin to fit the noise inherent in the data. Once over-fitting occurs, the model will have difficulty predicting new observations. The value  $Q^2$  is used to measure how well testing data generated by cross-validation is explained by the model.  $Q^2$  is calculated by randomly extracting rows from the  $X$  matrix to use as testing data. A PCA model is built on the remaining  $X$  matrix, then the scores, predicted values, and residuals of the extracted row is determined. This process is repeated until each of the rows has been extracted, one at a time. A new, cross-validation, residual matrix is formed,  $E_{A,CV}$ , and the overall  $Q^2$  is then determined from equation (15) [4].

$$Q_A^2 = 1 - \frac{Var(E_{A,CV})}{Var(X)} \quad (15)$$

Both  $R^2$  and  $Q^2$  are always less than one; and  $Q^2$  is always less than  $R^2$ .  $R^2$  will continue to increase with each successive component;  $Q^2$  will begin to decrease after a certain number of components, signalling over-fitting. However, Dunn recommends using cross-validation as a guide, and the number of components used should be judged on the relevance of each component depending on the intended use of the model [4].

Wallace used PCA on the measured temperatures and z-axis thermal drift to “ensure coherent data correlation between the process and quality data” [3]. The loading plot indicated that as temperature increased the z-axis moved downward, allowing for compensation of the thermal errors [3]. However, PLS was then used to relate the temperature measurements as a prediction tool for z-axis thermal drift.

Wallace also used PCA to model good process data against a training set of good process data from the same day, a different day, and simulated process fault experiments of a slightly crooked part due to residual chips from a previous cut [3]. The  $X$  matrix consisted of the data outlined in Table 4 in 2.3.2. The PCA model was effective at capturing the main effects of the process, verifying good parts, and detecting an actual non-catastrophic event of a part mis-load [3].

However, it was not sensitive enough to detect minor faults performed during experimental simulations [3].

### 2.3.3.3 Projection to Latent Structures

Projection to Latent Structures (PLS) is also used to find the latent variables and residual error; however, in this case the latent variables must not only explain the variance in  $X$ , they must simultaneously be correlated with a response matrix  $Y$  [33]. In process monitoring,  $Y$  commonly refers to a matrix of quality outcomes for each observation, such as measured feature on a part, or a good or poor product quality rating. The objective functions for PCA and PLS are shown below:

- PCA: maximize the variance in  $X$
- PLS: maximize the covariance between  $X$  and  $Y$

The NIPALS algorithm for PLS, as adapted from Dunn, is stated below [4]. It proceeds similar to that of PCA, except that the iterations are performed through both  $X$  and  $Y$ .

1. Data pre-processing of raw  $X$  matrix: mean-center and scale data to unit-variance.
2. Create an initial column of scores, now referred to as  $u$ , by selecting a column of  $Y$ .
3. Take every column in  $X$ , and regress it onto  $u$ , and store the regression coefficients as the loadings, now referred to as  $w$ .

$$w_a = \frac{1}{u_a^T u_a} X^T u_a \quad (16)$$

Columns in  $X$  that are strongly correlated with  $u$  will have large weights in  $w$ , while unrelated columns will have small weights.

4. Normalize the weight vector to unit length:

$$w_a = \frac{1}{\sqrt{w_a^T w_a}} w_a \quad (17)$$

5. Regress every row in  $X$  onto the weight vector,  $w$ , and store the coefficients in  $t$ .

$$t_a = \frac{1}{w_a^T w_a} X_a w_a \quad (18)$$

6. Regress every column in  $Y$  onto the score vector  $t$ , and store the slope coefficients in  $c$ .

$$c_a = \frac{1}{t_a^T t_a} Y_a^T t_a \quad (19)$$

7. Regress every row in  $Y$  onto the weight vector,  $c$ , and update  $u$

$$u_a = \frac{1}{c_a^T c_a} Y_a c_a \quad (20)$$

8. Iterate steps 3 to 7 until the change in vector  $u$  from one iteration to the next is small, usually  $10e-6$  or  $10e-9$ .
9. On convergence, store the final vectors:  $w_a$ ,  $t_a$ ,  $c_a$ ,  $u_a$ . These values represent the latent variable of principal component  $a$ .
10. Deflate to remove the variability already explained in  $X$  and  $Y$ :

- a. Calculate a loading vector for the  $X$  space.

$$p_a = \frac{1}{t_a^T t_a} X_a^T t_a \quad (21)$$

In this case, the loading vector  $p$ , was actually calculated after convergence; thus, it is not really a part of the PLS model. This is done because in the future when using the PLS as a prediction on new testing data, the  $Y$  matrix will not be available. Therefore,  $X$  must be a prediction of the  $t$  scores, since these will be available for new values of  $X$ .

- b. Remove the predicted variability in  $X$  and  $Y$ .

$$F_a = Y_a - t_a c_a^T \quad (22)$$

$$Y_{a+1} = F_a \quad (23)$$

11. Go back to step 2 and repeat the entire process for the next component until a satisfactory amount of variation has been modelled, without over-fitting the data.

Hussein used PLS to develop a model for surface roughness monitoring, and to apply model inversion techniques for process planning and quality improvement on a milling machine [1]. The  $X$  matrix consisted of the data outlined in Table 4 in 2.3.2 and cutting parameters of feed per tooth, depth of cut, and speed; the  $Y$  matrix was the quality of the machined surface, represented by a surface finish value  $Ra$  [1]. Tests were carried out on sharp tools, worn tools with 0.15 mm flank wear, and tools with breakage of 0.02 mm<sup>2</sup> [1]. Multivariate models were able to successfully differentiate between the different test conditions and to predict surface roughness [1].

Wallace's PLS model of temperatures and z-axis thermal drift was applied for real time thermal error compensation [3]. Wallace concluded that although the part data was noisy, the PLS model was able to eliminate most of the variability and determine the general trend of thermal distortion of the machine [3].

Wallace also used a PLS model to predict part quality data from process data [3]. A model including 84 observations resulted in a low predictive ability; however, all of the predictions were within the specified tolerance limits given [3].

### **2.3.3.4 PCA versus PLS**

Both PCA and PLS models can be used for multivariate process monitoring. ProSensus recommends using PCA when there are no quality measurements, or when the quality measurements are inadequate; and using PLS when the quality outcomes are well defined, so the model will be more sensitive to the quality-related outcomes [33]. However, the selection of PCA versus PLS is subject to the specific application; for example, Nomikos and MacGregor selected PCA even when the quality information was accessible [34], to be discussed in section 2.4. According to Dunn, a PCA model will pick up a greater scope of alarms related to process data and quality than a PLS model on the same  $X$  [35]. This is because PCA represents only  $X$ , whereas PLS has to represent  $X$ ,  $Y$  and the covariance between  $X$  and  $Y$ . The projection of the raw data onto the PCA plane will not always be the same as projection onto the PLS plane. Since the PLS plane is orientated to include  $Y$ , it can miss out on some alarms in the  $X$ -space [35]. Therefore, PCA is the predominate multivariate technique used in process monitoring [35]. However, one must select the modelling technique that is best suited for the specific application and carefully analyze the results.

## **2.4 Decision Making Strategy**

Prior to implementing online process monitoring, as outlined in Figure 1, an offline multivariate model must first be created. This offline model is built on

a substantial amount of process and quality data collected during machining. This data is referred to as the training set. The training data set specifies the correlation structure inherent in the data. The multivariate model created from the training set is used to set the statistical process control limits. Once these limits are established, the data from the training set can be stored offline, and only the limits are retained for online monitoring.

Nomikos and MacGregor successfully developed multivariate statistical process control charts for online monitoring of the progress of new batches to facilitate analysis of operational and quality-control problems in a chemical engineering application [34]. Nomikos and MacGregor used the following guidelines for establishing control charts [34]:

1. The reference distribution, or training set, should be based on a history of past successful normal observations against which future observations can be compared. This reference distribution should contain only those observations considered to be from common-cause variation; and all observations exhibiting unusual characteristics should be omitted.
2. Build a multivariate PCA model based on the reference distribution.
3. Select the number of principal components based on the various methods available. Do not be alarmed by low  $R^2$  or  $Q^2$ . A  $R^2$  of 55%, for example, is to be expected when dealing with large data sets.

4. Construct the control charts to monitor the  $t$  scores and the error for new observations.

The  $t$  scores can be easily monitored by use of the Hotelling's T2 statistic. A large Hotelling's T2 statistic represents that a new observation is operating in the same way as the observations in the training set, but has a larger than normal variation in the measurements. The error can be monitored by use of the squared prediction error (SPE) statistic. A large SPE value represents that a new observation has a fault that was not evident in the training set. A SPE versus Hotelling's T2 plot with control limits defined by the training set is a useful control chart for detecting both types of errors.

### 2.4.1 Hotelling's T2

Hotelling's T2 statistic (HT2), usually pronounced as Hotelling's T-squared, is computed using the scores of the model and is given by equation (24); where  $i$  is the observation number and  $a$  is the component [33].

$$T_i^2 = \sum_{a=1}^A \frac{t_{i,a}^2}{s_{t_a}^2} \quad (24)$$

The HT2 critical limit at significant level  $\alpha$  is shown in equation (25), as adapted from Kourti and MacGregor; where  $N$  represents the number of observations,  $A$  represents the number of components,  $F_\alpha$  the F-distribution with degrees of freedom of  $A$  and  $N-A$  [36].

$$T_{\alpha}^2 = \frac{(N-1)(N+1)A}{N(N-A)} F_{\alpha}(A, N-A) \quad (25)$$

The HT2 limits are commonly shown on HT2 plots at significance level  $\alpha$  at 95% and 99%, representing the two and three sigma confidence limits, respectively. When a new observation is above these limits, it may be assumed to be an outlier.

### 2.4.2 SPE

Squared prediction error (SPE) gives a quantity of how well the observation belongs to the model [33]. A high SPE value means that the observation lies off the model plane created by the principal components. A high SPE can occur when the observation represents a correlation structure that differs from that of the training set. In this case, the model cannot accurately represent the new observation. The SPE is calculated as the sum of squares across the residuals,  $E$ , of each observation, denoted  $i$ , shown in equation (26), where  $k$  is the variable index, and  $K$  is the total number of variables [33]. The residuals account for any disturbance that is not described sufficiently in the data base of good observations, and this makes them very sensitive in detecting new faults [34].

$$SPE_i = \frac{\sum_{k=1}^K E_{ik}^2}{K} \quad (26)$$

The SPE critical limit at significant level  $\alpha$  is shown in equation (27); where  $v$  is the sample variance and  $m$  is the sample mean of SPE, and  $\chi^2$  is the critical value of the chi-squared distribution [34].

$$SPE_{\alpha} = \left( \frac{v}{2m} \right) \chi_{\frac{2m^2}{v}, \alpha}^2 \quad (27)$$

Similarly to HT2, the SPE limits are commonly shown on SPE plots at significance level  $\alpha$  at 95% and 99%, representing the two and three sigma confidence limits, respectively. When a new observation is above these limits, it may be assumed to be an outlier.

### 2.4.3 Outliers

In the application of process monitoring, the occurrence of outliers from either a high HT2 or SPE value, requires usage of a decision making strategy with options such as:

- A. immediately stop production,
- B. investigate problem while production is online, or
- C. ignore.

This decision can be based on an examination of the variables that lead to the outlier. Contributions to scores, given by equation (28), or SPE, given by equation (29), compare how the selected observation differs from the average of the other observations.

$$\text{Score Contribution}_k = (X_{to} - X_{from}) \sqrt{\sum_a \left( \frac{T_{to} - T_{from}}{S_{t_a}} \right)^2} P_a \quad (28)$$

$$\text{SPE Contribution}_{i,k} = E_{i,k}^2 \times \text{sign}(E_{i,k}) \quad (29)$$

$$\text{Where, } E_{i,k} = (X_{i,k} - T_{i,l:A} P_{k,l:A}) \quad (30)$$

Contributions can be used to find which variable contributed in causing the observation to differ from the others. With time and knowledge, the contributing variables can start to be correlated with occurrences in the process and the final product quality. For example, a contributing variable of higher than average acceleration may indicate an out of balance spindle. The end result can be a process monitoring control plot that highlights the likely cause of a new observation being an outlier. This information can then be used to allow the technician to take the appropriate action.

#### 2.4.4 Process Control Confidence

The level of confidence of a process monitoring system can be measured by type I and type II error. A type I error occurs when a sample of normal operation falls outside of the control limits [4]. Type I error can also be referred to as a false alarm, a false positive, and producer's risk [4]. Assuming central limit theory applies, and the data represents a normal distribution, which is commonly true for data sets with over 30 observations, the probability of making a type I error is given by equation (31). Given a confidence limit of 95 and 99%,

the probability of type I error is 5 and 1%, respectively. This means that given 100 common-cause observations, it is likely that at least 1 observation will lie outside of the 99% confidence limit.

$$P_{\text{Type I Error}} = 100 - \alpha \quad (31)$$

A type II error occurs when an abnormal sample falls within the control limits [4]. A type II error can also be referred to as a false negative or consumer's risk [4]. The probability of a type II error is a function of the degree of abnormality in the data [4].

Either error rate can be determined by simply summing the number of errors and dividing by the total number of observations predicted. Process monitoring models with minimal error rates increase the confidence of these techniques. However, minimal error rates is a subjective term and needs to be decided based on the specific application and the cost of error.

A process monitoring system that begins to experience an unusual amount of false alarms, or observations that hover around the 95% confidence limit, is indicative of a need for calibration. Calibration is required when there is a phenomenon occurring in the system that was not represented by the historical data set used to build the training set. This can occur when the model is very new and the historical set did not include enough information, or when the system has experienced changes over a time period that shift the correlation structure, such as machine maintenance or ambient conditions.

## 2.5 Process Monitoring Areas of Improvement

This literature review presented examples of work completed in academia and industry on the topic of process monitoring and multivariate analysis. However, much of this research focused on the use of individual sensors, applications in the chemical industry, or areas where there is room for improvement. The research discussed shows promise for online process monitoring in the manufacturing industry. The goal of this research is to bring together all of the knowledge learned thus far to create an online process monitoring system for discrete part manufacturing, which utilizes multivariate analysis. This will be done by continuing with the work of Hussein, Ruparelia and Wallace, by addressing some of their recommendations for future work [1,2,3]:

- Hussein
  - Apply to turning system
  - Perform tests on additional faults
- Ruparelia
  - Relate signals to quality measures
  - Selection of monitoring frequencies based on specific setup
- Wallace
  - Increase signal to noise ratio
  - Consider more of the frequency spectrum

## **Chapter 3 - Experimental Methods**

### **3.1 Introduction: Laboratory versus Industrial Testing**

Prior to beginning industrial testing, sensor equipment was installed in the MMRI on an Okuma Crown L1060 lathe. The goal was to run testing conditions to prepare, plan and execute process monitoring in a controlled environment to establish confidence with the sensor setup and the process monitoring concepts. The tests simulated changes in the cutting zone by altering cutting parameters and other cutting conditions. A discussion of the setup and analysis of tests completed in the MMRI laboratory will be discussed and analyzed in Chapter 4. Following this, Chapter 5 will discuss the details surrounding the industrial tests, including the manufacturing process being analyzed, as well as the successes and challenges of process monitoring in industry as compared to the laboratory. The instrumentation, data acquisition and analysis methods discussed in this chapter apply to both the laboratory and industry tests.

## **3.2 Instrumentation**

### **3.2.1 Current Sensor**

In addition to the benefits stated in section 2.2.1 regarding use of current sensors, with the assistance of a skilled electrician, current sensors can be quickly and easily installed on a machine. It is recommended to have an electrician mount the sensors, since the electrical panel must be accessed. The main lines supplying the motor must be disconnected to feed through the sensors, and then reconnected. This process can take as little as a couple of minutes, allowing the machine to quickly resume production. In a machine with a three phase AC motor, it is only necessary to apply the current sensor to one phase, since each phase has the same peak to peak amplitudes, but are just displaced by  $120^\circ$ .

Three closed loop Hall Effect current sensors, model CLSM-100LA from Sypris Test and Measurement, were mounted in the electrical panel. Figure 4 shows one of the current sensors mounted on the main power line of the spindle motor. The other two current sensors are mounted on the X and Z axis power lines.

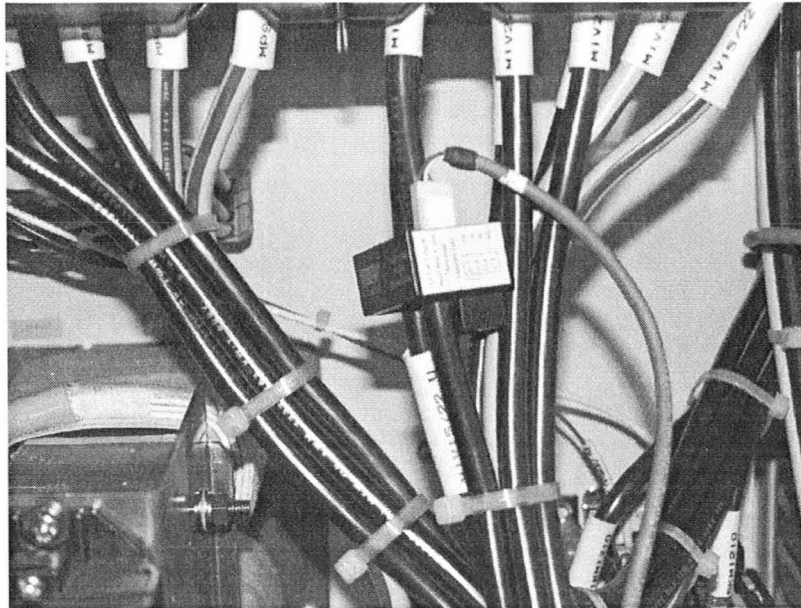


**Figure 4: Spindle Current Sensor**

These current sensors measure AC and DC currents within a range of 0 to  $\pm 200$  A, have a sensitivity of 1 A in to 0.5 mA out, accuracy of 0.5 A, and response time less than 0.5  $\mu$ s. The signal condition box shown in Figure 5 was used to convert the current output from the current sensors into a voltage output to be read by the National Instruments NI USB-9215A. This data acquisition device has 4 channels of 16-bit each to simultaneously sample analog input. The maximum sampling rate of each channel is 100 kHz. The three resistors within the signal condition box were from Precision Resistor; model SM2812, with maximums of 5 W and 1000 V, and an accuracy of  $\pm 1\%$  of the full scale output.

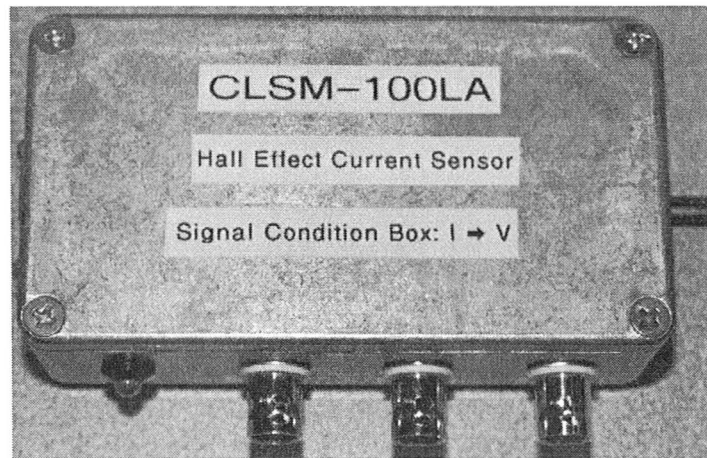


**Figure 5: Signal Condition Box for Current Sensors**

### **3.2.2 Accelerometer**

A Kistler accelerometer, model number 8702B50 was mounted on the spindle bearing housing as shown in Figure 6. The accelerometer has a range of  $\pm 50$  g, sensitivity  $\pm 100$  mV/g, a frequency range of 0.5 to 10,000 Hz, and a resonant frequency 54 kHz. The accelerometer requires a data acquisition device capable of taking frequency measurements from integrated electronic piezoelectric (IEPE) sensors, such as National Instruments device NI 9234. NI 9234 has four channels of  $\pm 5$  V, with a maximum sampling rate of 51.2 kHz per channel.

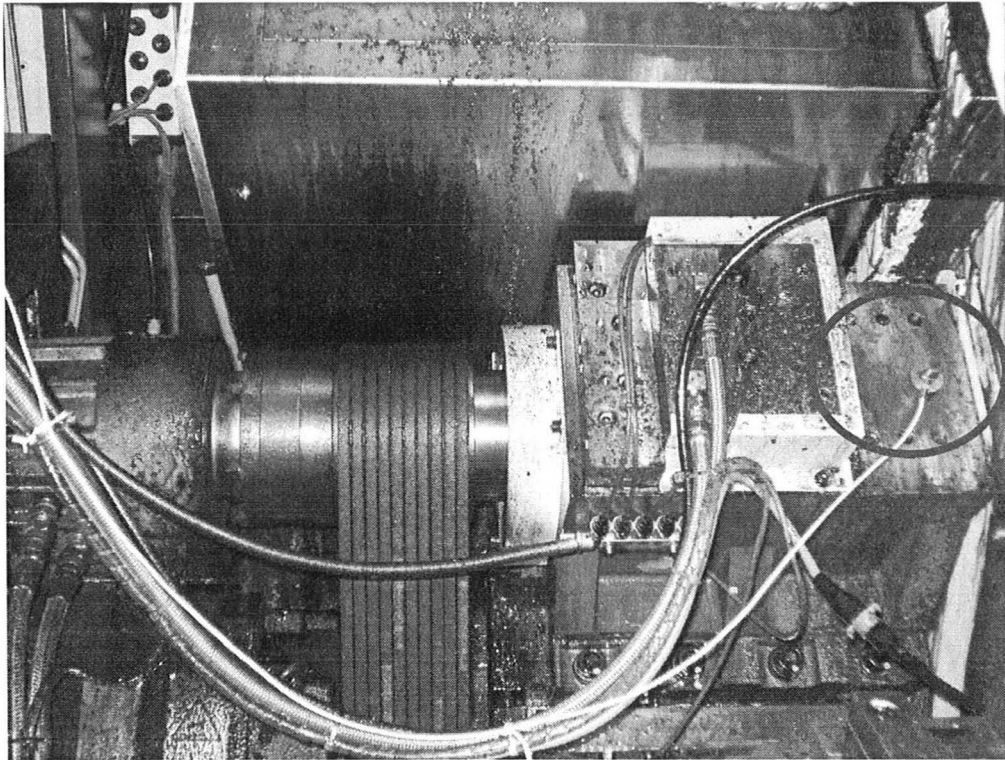


**Figure 6: Accelerometer mounted on spindle bearing housing of lathe**

Various methods can be employed to mount the accelerometer, including: stud mount, adhesive cement, and magnetic base. Table 5 outlines the advantages and disadvantages of each of the mounting methods. Magnetic base mounting was selected due to its quick and easy installation. Furthermore, shaker table testing of the accelerometer stud mounted versus magnetic mounted indicated that the mounting methods produce a similar output, with an error of only 3.5% for the frequency range examined.

**Table 5: Accelerometer mounting methods**

<b>Mounting Method</b>	<b>Remarks</b>	<b>Advantages</b>	<b>Disadvantages</b>
<b>Stud</b>	<ul style="list-style-type: none"> <li>- 10-32 stud</li> <li>- <math>2 \pm 0.2</math> Nm mounting torque</li> </ul>	<ul style="list-style-type: none"> <li>- Best coupling</li> <li>- Highest frequency response</li> </ul>	<ul style="list-style-type: none"> <li>- Requires threaded hole in specimen</li> </ul>
<b>Adhesive Cement</b>	<ul style="list-style-type: none"> <li>- Clean, smooth surface</li> <li>- Loctite, superglue</li> </ul>	<ul style="list-style-type: none"> <li>- Good coupling</li> </ul>	<ul style="list-style-type: none"> <li>- Difficult to remove sensor</li> <li>- Requires solvent</li> </ul>
<b>Magnetic Base</b>	<ul style="list-style-type: none"> <li>- Clean, flat surface</li> <li>- Ferromagnetic material</li> </ul>	<ul style="list-style-type: none"> <li>- Easy and quick installation</li> </ul>	<ul style="list-style-type: none"> <li>- Adds mass to loading</li> <li>- Lowers resonant frequency</li> </ul>

### 3.2.3 Thermocouple

Four thermocouples were mounted on the lathe to monitor changes in temperature. Mounting locations included: outer temperature of machine as a result of ambient and machine conditions, spindle bearing housing, coolant, and X motor housing, as shown in Figure 7.

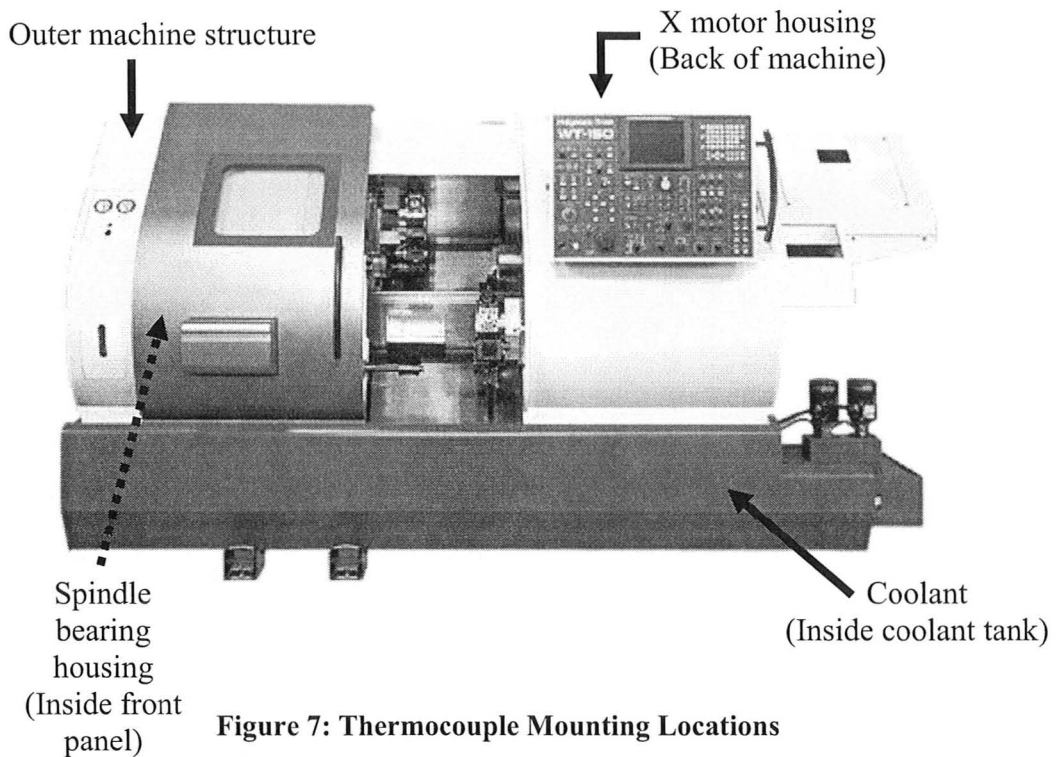


**Figure 7: Thermocouple Mounting Locations**

**(Image: Nakamura-Tome WT-150 [37])**

Surface thermocouples with self-adhesive backing of type T were used from Omega, model number SA1-T-120, for the three dry measurements. A hermetically sealed type T thermocouple was used for the coolant measurement, also from Omega, model number HSTC-TT-120. The type T thermocouples are rated for measurements between -200 to 350 °C, and have better than 0.3 s response time. Data acquisition was completed on NI 9219, a 24-bit universal analog input device. NI 9219 can be used for thermocouple measurements at sampling rates of 50 Hz per channel; and RTD, resistance, voltage, and current

measurements, with sampling rates of 100 Hz. The advantage of using NI 9219 for thermocouple measurements is a per channel built-in thermistor for cold-junction compensation calculations; however, it is important for the device to be in a stable temperature environment and away from any heat sources.

### **3.3 Data Acquisition**

As previously discussed, all data acquisition (DAQ) was performed with National Instruments devices. Each DAQ device was paired with its own C Series USB Single Module Carrier, model NI USB-9162, resulting in three separate USB DAQ devices. Multiple carriers were used so data from each sensor could be acquired at different sampling rates. For example, it is unnecessary to sample temperature at as high a rate as vibration. For applications in which precise timing is pertinent, investment in a USB carrier, with connections for multiple devices with different sampling rates would be more desirable. However, at the time of this research, this type of unit was not yet available from National Instruments.

Data acquisition was performed in LabVIEW using three separate DAQ Assistant Express Virtual Instruments for each of the DAQ devices. LabVIEW was well suited for data acquisition because it allows for quick and easy setup and works seamlessly with NI devices. MATLAB could not be used for data acquisition as features on many of the NI DAQ devices were not yet supported by

MATLAB 2009b. MathWorks suggested that future MATLAB versions will support more of National Instruments device capabilities.

### **3.3.1 Sampling Frequency**

It is difficult to know the frequency of interest in process monitoring applications, as it can change with disturbances in the process. However, one easily determined frequency of interest is that of the spindle RPM. Dividing the spindle RPM by 60 will yield a frequency value in hertz, which can be detected by a spectral analysis. So at minimum, the sampling frequency should be at least two times this value, according to Nyquist. However, in most applications, the RPM frequency is much lower than that of the DAQ devices and sensor specifications. In the case of the current sensor, a common sampling frequency of 10 kHz was selected. The accelerometer, which signal was to be analyzed by use of the FFT, required following some of the recommendations outlined in section 2.3.1. Since all the frequencies of interest were unknown, focus was placed on the maximum signal of 10 kHz detectable by the accelerometer. Thus, assuming 10 kHz was the frequency of interest, and considering the Nyquist frequency and the power of two rule,  $2^{15}$  or 32768 Hz should be selected. However, a sampling rate of 32768 Hz leads to a problem when dealing with the accelerometer DAQ device NI 9234, because sampling rate selection must obey an equation defined by the internal master time base on the device. Acceptable sampling rates are

given by equation (32), where  $F_s$  represents the sampling rate, and  $F_m$  represents the frequency of the internal master time base [38].

$$F_s = \frac{F_m / 256}{N} \quad \text{where } N = 1 \dots 31, F_m = 13.1072 \text{ MHz} \quad (32)$$

Therefore, accelerometer sampling rates range from a maximum of 51.2 kHz, followed by 25.6 kHz, to a minimum of approximately 1650 Hz, none being equivalent to a power of two.

Given the selection of available sampling rates, the maximum sampling rate of 51.2 kHz was selected as the accelerometer sampling frequency. Since zero-padding can lead to misleading results, it was decided that zero-padding would not be done, and the FFT efficiency would have to rest on the computer processor instead of the power of two suggestion. Aliasing will likely be avoided since NI 9234 has a built-in anti-aliasing filter that automatically adjusts to the selected sampling rate. The anti-aliasing filter functions as follows [38]:

1. ADC samples at 128 times the sample rate selected, up to  $F_m$
2. A digital filter expands the data to 24 bits and rejects signal components greater than 12.5 kHz (Nyquist Frequency)
3. Data is digitally re-sampled at original sample rate

Use of a high quality DAQ device coupled with appropriate sampling rate selection should aid in yielding accurate and repeatable vibration data during experimentation.

Finally, since indirect temperature measurements tend to move slowly, a sample rate of 1 Hz will be adequate for the thermocouples.

Tests performed in the MMRI were sampled at the mentioned sampling rates for three seconds to increase the frequency resolution. However, in the industrial tests, the process was so fast, that less than one second of sampling was available.

### **3.3.2 Serial Port Trigger**

In the controlled tests completed in the MMRI laboratory, data acquisition was easily triggered manually, and the steady-state portion of the data which excluded the initial plunge and final extraction was manually selected. However, the industrial machining process involved many steps, which happened extremely quickly. The overall process was loud and difficult to observe, and as a result, nearly impossible to manually trigger data acquisition at the correct point in the process. Furthermore, collecting data for the entire process generates large quantities of data that would be hard to sort through; and at the current sampling rates and computer speed, LabVIEW will only acquire data for ten seconds. To resolve this issue, a serial port trigger was utilized. Serial ports on CNC machines

are commonly used for loading or storing programs between the CNC machine and a storage device such as a computer. Figure 8 shows a schematic of the connection between the machine and the laptop being used for data acquisition. The null modem cable was purchased from Allied Electronics, and the serial adaptor cable from Dell.

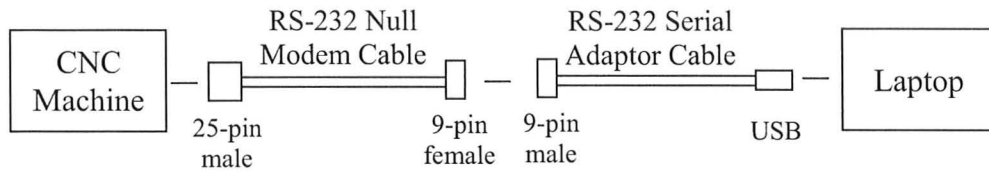


**Figure 8: Serial Port Communication Cabling Schematic**

Depending on the FANUC version on the CNC machine various parameters must be set. Appendix A lists the required parameter settings, as adapted from the FANUC parameter manual for the MMRI Nakamura-Tome SC450, FANUC version 21-TB, using RS-232 port 0 [39].

The CNC code for serial port communication uses the ‘DPRNT’ command. This function sends information from the CNC machine out through the RS-232 port. The following code shows the port being opened, the letter “A” being sent, and the port being closed.

```
POPEN;  
DPRNT[A];  
PCLOS;
```

In order for the DPRNT command to be successful, the computer must be open to receiving. This means that all of the parameters must match and a program be used to acquire the sent information. LabVIEW Instrument I/O Assistant was used to receive the DPRNT signal. The Instrument I/O Assistant was placed within a case structure, inside a while loop, with an indefinite timeout, so that LabVIEW would essentially sit 'idle' waiting for a signal from the CNC machine. Once the signal was received, the Instrument I/O Assistant would finish execution and the data acquisition case structure would begin. This cycle would repeat until the user selected to terminate the while loop. Each cycle collected process data corresponding to a critical feature being machined automatically, without the need for any manual intervention.

### **3.3.3 Data Acquisition Sample**

Figure 9 shows an example of the data collected for one observation in the MMRI laboratory tests from the current, accelerometer and temperature sensors, respectively. Note that the scales on the graphs are different in order to observe the signal.

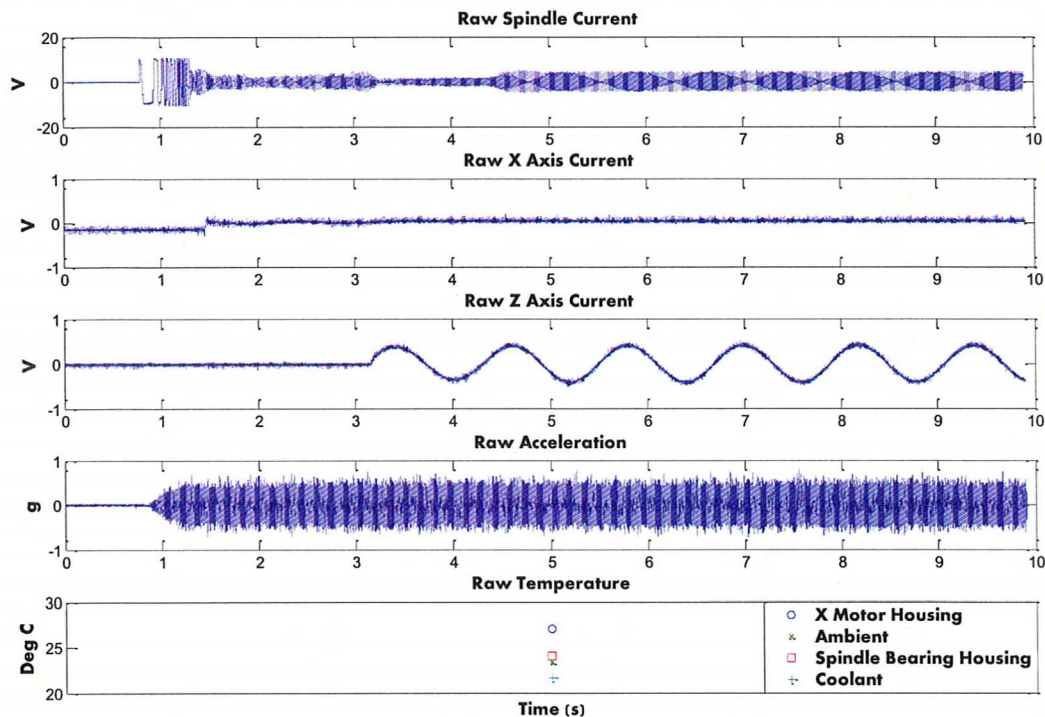


**Figure 9: Raw Data Sample**

The signals shown in Figure 9 represent the following machining sequence: spindle on, movement in X and Z toward workpiece, plunge, and cutting. Data acquisition stopped before cutting was completed. The steady state cutting region used for data processing was a region between approximately six and nine seconds.

### 3.4 Data Processing

Prior to performing MVA, the signals acquired during data acquisition were processed in an attempt to compress the data into a manageable size while

still maintaining the important information collected during machining. The RMS of each of the current sensors signals was chosen to represent this information. As shown in Figure 9, the current signals of the active motors, both spindle and Z, produce sinusoidal waveforms. The frequency of these waveforms is proportional to the motor speed. However, the spindle motor speed will always be set by the user and programmed into the G-code, so monitoring the frequency of current is not relevant as it should never change. Instead the magnitude of the current is important since it is representative of the forces experienced during machining as discussed in Section 2.2.1.

Unlike the current signals, the accelerometer waveform was much more complicated. As discussed previously, this type of signal is commonly analyzed using the FFT.

Initial sensor data was analyzed by means of averaging multiple FFT's as discussed in 2.3.2. However, it was determined that considering the entire spectrum improved the frequency resolution, which likely decreased the spectral leakage, outweighing the benefits seen by averaging.

Figure 10 shows the FFT of the accelerometer signal from Figure 9, within a range of 0 to 10,000 Hz, the maximum detectable frequency of the accelerometer.

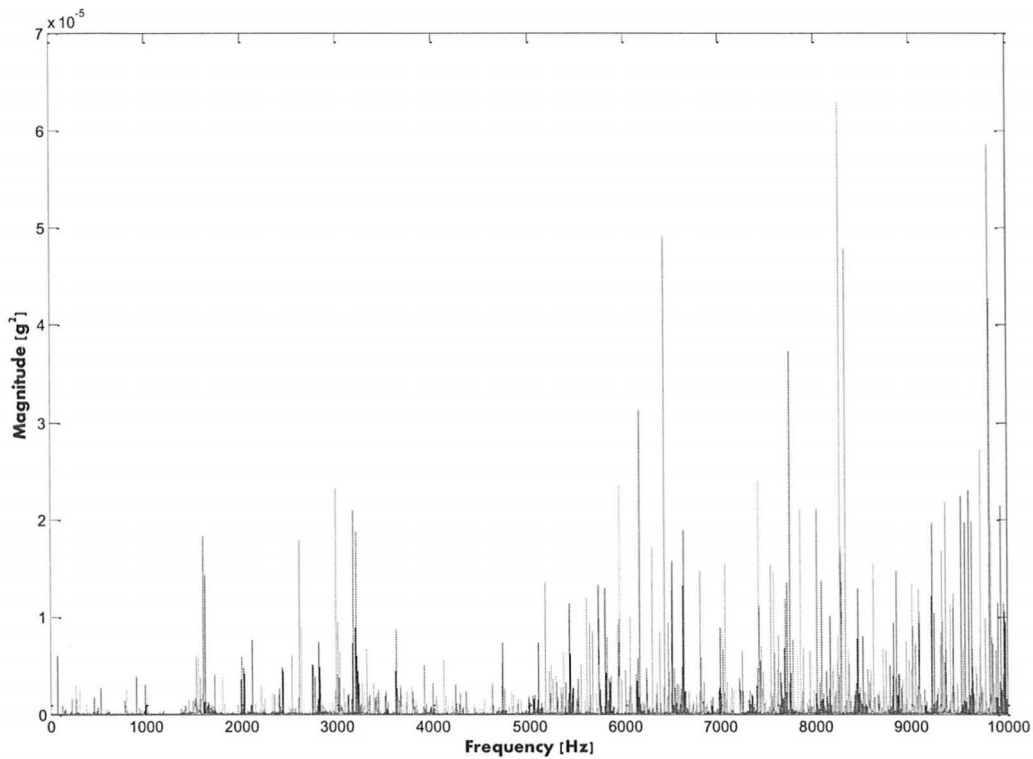


**Figure 10: Results of Accelerometer FFT**

Recall that Wallace saved only the FFT magnitude at the tooth passing frequency, and Hussein the maximum within the frequency band of 2 kHz, although he was examining the FFT of the force signal [3,1]. However, Wallace did mention that there is likely much more information within the entire frequency spectrum, but had difficulty with data storage capabilities [3]. To retain more of the frequency information, the frequency domain was divided into regions of frequency of 100 Hz. For each 100 Hz region, the maximum magnitude was found, as well as its corresponding frequency. Results of this

processing method for the FFT data in Figure 10 are presented as a bar chart in Figure 11.

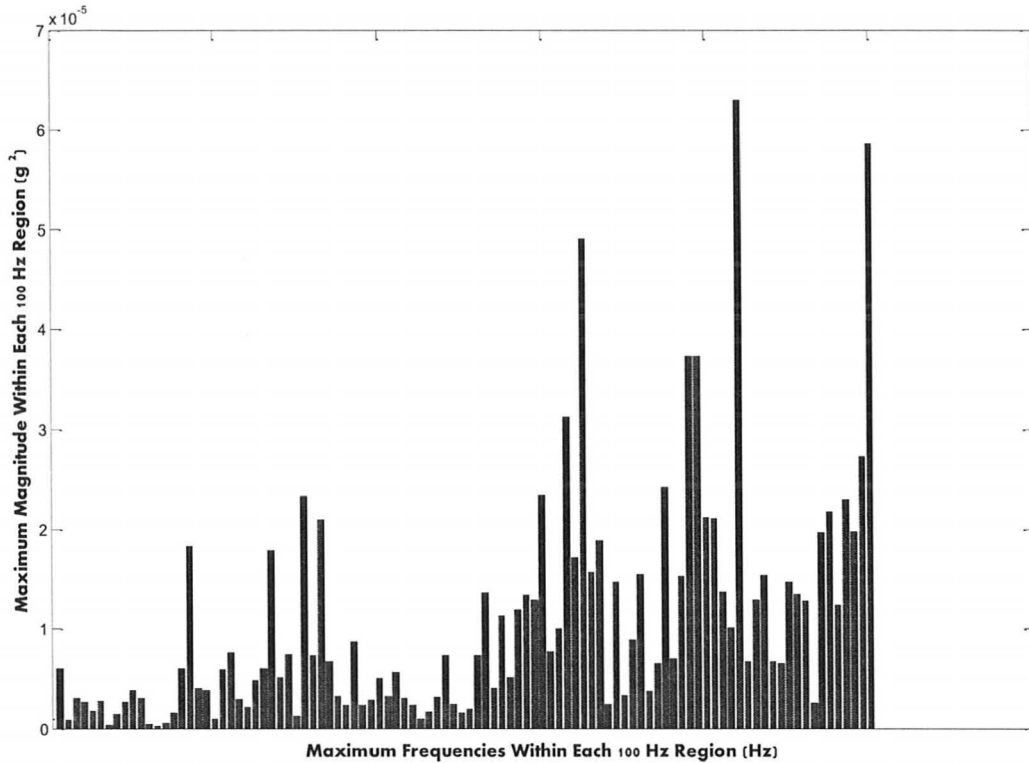


**Figure 11: Results of Processed Accelerometer FFT**

The overall shape of the FFT data is still present except that there are only 100 frequency values to consider instead of 10,000. It is important to retain both the maximum magnitude and the frequency at which the magnitude occurred. With further testing and experience one could start to relate frequencies with specific events within the machine. For example, the bearings likely have an excited frequency based on the number of balls within the bearing.

Since temperature is relatively slow moving, the single temperature reading collected during data acquisition will be considered and no further processing is required. Table 6 presents a summary of each of the acquired sensor signals, the processing method, and the variable notation.

**Table 6: Data Processing Methods for Sensor Signals**

<b>Signal</b>	<b>Data Processing</b>	<b>Resulting Variable Notation</b>
Spindle current	RMS	RMS <sub>s</sub>
X-axis current	RMS	RMS <sub>x</sub>
Z-axis current	RMS	RMS <sub>z</sub>
Acceleration	100 Hz bands based on FFT RMS	f1, f2,...f100, m1, m2,...m100 RMS <sub>acc</sub>
X-axis motor temperature	Raw data	Temp <sub>x</sub>
Ambient temperature	Raw data	Temp <sub>am</sub>
Spindle temperature	Raw data	Temp <sub>s</sub>
Coolant temperature	Raw data	Temp <sub>cool</sub>

Once the sensor data was processed, the resulting  $X$  matrix contained a total of 208 columns, which included: three current RMS values, 200 frequencies and magnitudes, one accelerometer RMS, and four temperatures. The number of rows was equal to the number of observations collected in the different testing situations. This  $X$  matrix was then inputted into the multivariate algorithm.

### 3.5 Multivariate Analysis

#### 3.5.1 ProMV versus MATLAB

ProSensus' ProMV software was used for offline multivariate analysis because of its ease of use, in terms of a graphical user interface which allows for

testing of different modelling techniques, ability to view many graphs, and options for selecting certain observations to examine their contribution plots. Recall that contribution plots allow investigation into what variables resulted in a certain observation being different from the average.

However, it was important to be able to replicate these multivariate models in MATLAB for future use in online applications. Utilizing MATLAB would bring this research one step closer to having a commercially available online monitoring system to acquire new data, process the new data, compare the new data to a previously built multivariate model, and output predictions of part quality. This is not currently possible with commercially available multivariate software such as ProMV or even Simca-P.

The MATLAB multivariate code was verified with a testing data set from Dunn with known scores and loadings, presented in Table 7 [8]. The MATLAB multivariate code exactly matched Dunn’s scores and loadings to the fourth decimal place. ProMV matched Dunn’s results to the second decimal place. Therefore, the MATLAB code is accurate, but may differ very slightly from ProMV.

**Table 7: Raw Data, Scores and Loadings for Model Comparison  
(Adapted from [8])**

Raw Data	$X = [3, 4, 2, 2; 4, 3, 4, 3; 5, 5, 6, 4]$
Scores	$T = [-1.6229, 0.6051; -0.3493, -0.9370; 1.9723, 0.3319]$
Loadings	$P^T = ([0.5410, 0.3493, 0.5410, 0.5410], [-0.2017, 0.9370, -0.2017, -0.2017])$

### **3.5.2 Model Building: Training & Testing Data**

The guidelines of Nomikos and MacGregor presented in section 2.4 were followed in order to build the multivariate models. A data set representing data from standard operation was used to form the training set for a PCA model. A few observations from standard operation were with-held for testing, as well as observations representing disturbances or poor quality parts. The models were built in ProMV and MATLAB to ensure that either method produced the same results. The results from ProMV will be presented.

### **3.5.3 Model Analysis**

The topics presented in 2.4, regarding the decision making strategy was used for model analysis; this includes use of the SPE versus HT2 plot and contribution plots. ProMV was used for analysis due to its simple graphical user interface.

## **Chapter 4 - MMRI Laboratory Testing**

### **4.1 Introduction to MMRI Laboratory Testing**

The MMRI laboratory tests focused on three distinct features to be examined with process monitoring. These features were selected because they were easy to simulate in the laboratory and represented events that may occur in an industrial setting. Test A considered random disturbances during the cutting process, the disturbances included: unusual surface, an out of balance spindle, and coolant versus no coolant. Test B considered changes in depth of cut. Changes in depth of cut have the potential to represent operator error, oversized barstock, or missing operations. Finally, Test C considered machining with a new tool versus a tool with significant wear. While some of these test sets may not necessarily impact product quality, they represent easily applied, realistic occurrences in the machining process. Capability to detect these occurrences will increase the confidence surrounding the possibility of machine process monitoring.

The material used was raw barstock of mild steel that was cut down into three lengths of approximately 170 mm each. The length of barstock was held in the chuck at the midpoint, with material to be machined on either side. Turning tests were performed on one side, and then the barstock was flipped, so that the other side could be used. These smaller barstock lengths were used because they

were more manageable, and so that minimal to no change in vibration would occur when machining further away from the chuck. This demonstrates the diligence with which the tests were planned and implemented. Confounding effects were controlled as much as possible. Each of the tests sets, A, B and C, had constant surface speed, feed and depth of cut. Test A used the workpiece at its largest diameter; then Test B was used after A passes were complete, followed by C. This increased testing efficiency, while keeping the RPM for each set controlled. To account for varying temperatures in the machine from the start of a testing cycle to the end, from the ambient conditions from the morning to the evening, and the extremely hot summer season in Hamilton, Ontario during the experimentation, groups of tests were taken at random time periods. For example, three sets of A, B and C may be taken, followed by the next group later that day, or the next. 24 tests of each set were taken over the period of approximately one month. All timestamps were recorded. Testing parameters were based on a finishing operation used by GMI. These parameters will be referred to as the standard machining parameters. The standard machining parameters resulted in very minimal tool wear. Tool wear was monitored, and the insert was replaced periodically to ensure that tool wear was not confounding the results.

## 4.2 Test A – Simulate Disturbances

Test A included 20 tests using the standard machining parameters. For two tests, the surface to be machined was ‘roughed’, by hand, with a file. Although, this may not affect the finished surface quality, it does represent a change in the original surface, which has the potential to represent a change in the overall material. Catching incorrectly loaded material into the barstock feeder could be advantageous. To simulate an out of balance spindle, a bolt and nut was placed in a hole on the spindle housing as shown Figure 12. Finally, the coolant was turned off for one test; all other tests utilized coolant.

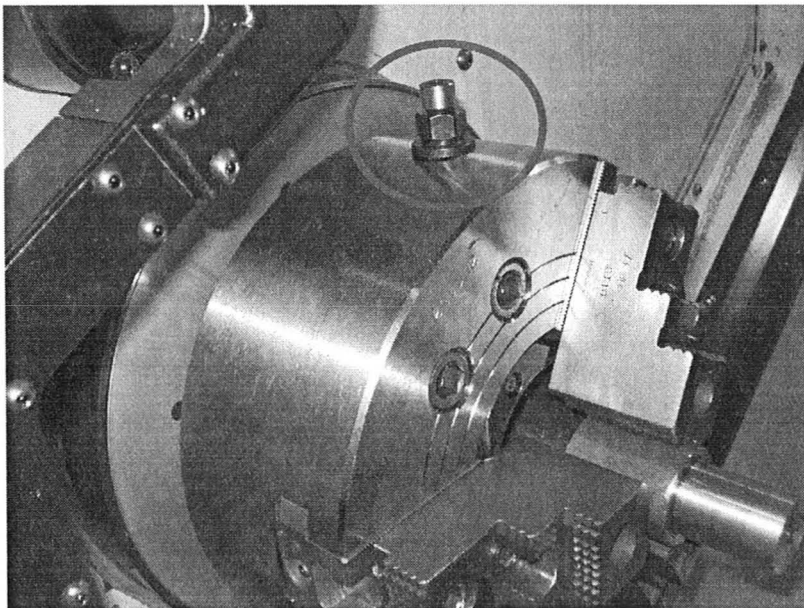


Figure 12: Spindle with bolt

### 4.2.1 PCA Model on All Variables

A multivariate model was built on the all 208 variables – 100 frequency and 100 magnitude values corresponding to the maximum FFT locations, 3 current RMS values, one accelerometer RMS value, and four temperature values. The observations shown in the first row of Table 8, corresponding to standard machining parameters, referred to as the training set, were used to build the model. The other observations shown in Table 8 correspond to the four disturbances and one standard observation withheld for testing purposes. A common mistake made is to randomly select ‘good’ observations for testing; however, a better representation of how the model will be used is to select the most recent ‘good’ observation for testing [8].

**Table 8: Test A Observations**

Observation Number	Description
1, 2, 10, 11, 12, 19, 21, 28, 29, 30, 38, 39, 47, 48, 55, 56, 57, 64, 65	Standard machining – training set
3, 20	Rough surface
37	Bolt
46	Coolant off
66	Standard machining – for testing

ProMV fitted a PCA model with 2 components and an  $R^2$  value of approximately 29%; meaning only 29% of the variability in the data was explained. The SPE versus HT2 plot is shown in Figure 13.

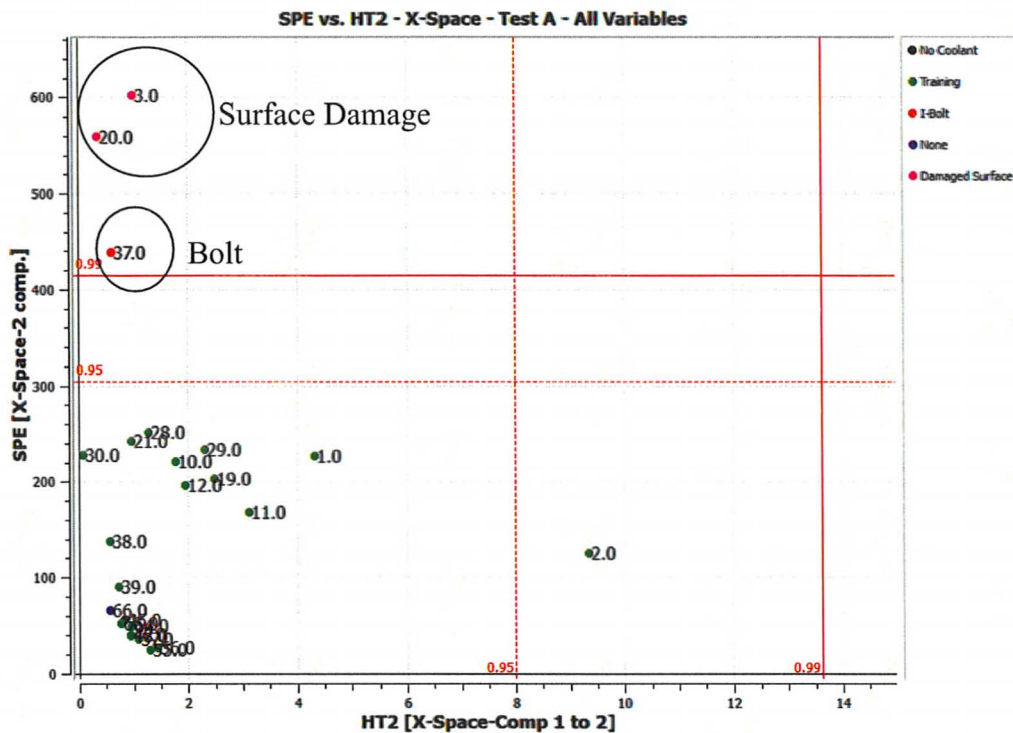
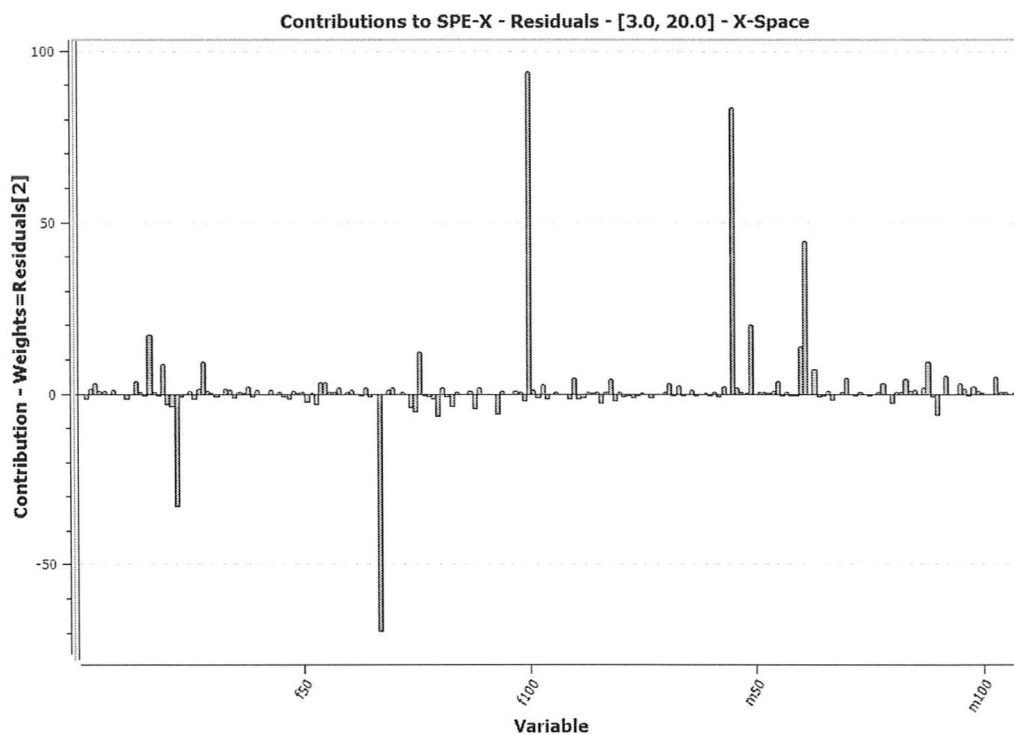


Figure 13: ProMV SPE vs. HT2 Plot for Test A

The control plot is able to isolate the disturbances 3, 20, and 37, but did not detect the coolant off condition. The control plot accurately represented observation 66 as a standard observation with the control limits. Contribution plots on each of the disturbances showed various frequency and magnitude variables as the contributing factors. Further investigation would be required to explain the reason behind the contributing frequency bands.

A contribution plot of the squared prediction error for observations 3 and 20, roughed surface, is shown in Figure 14; this plot illustrates the difficulty in

analyzing the results from the contributions of the 200 frequency and magnitude variables.



**Figure 14: ProMV Contribution Plot for Observation 3 and 20 from Test Set A**

Observation 2, which was from the standard machining parameters, was outside the HT2 95% control limit. Recall that an observation that does not fit within the HT2 limit, but is within the SPE limit, fits the model but has a larger variation in the measurements as compared to the other observations. A contribution in the score space of observation 2, Figure 15 and Figure 16, showed that the maximum variables were an order of magnitude smaller than that of the

other contribution plot examined; but did show an interesting result in terms of an increase in both Z current and temperature. The difficulty in seeing the final eight variables amongst the frequency and magnitude information suggests that perhaps these variables need to be considered in independent PCA models.

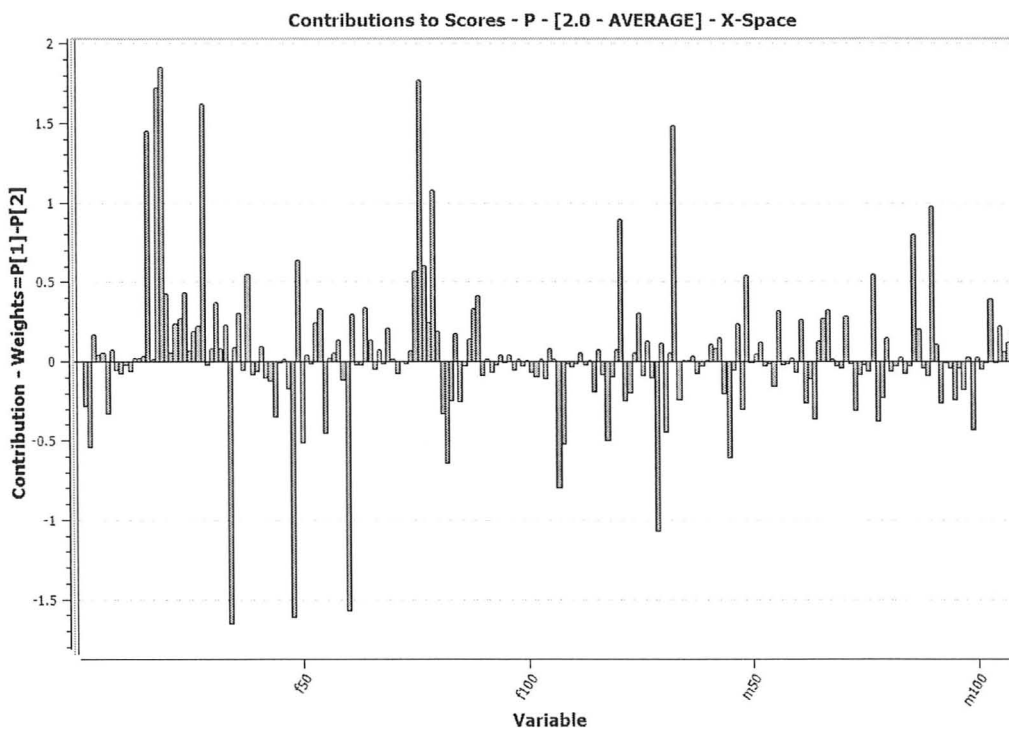
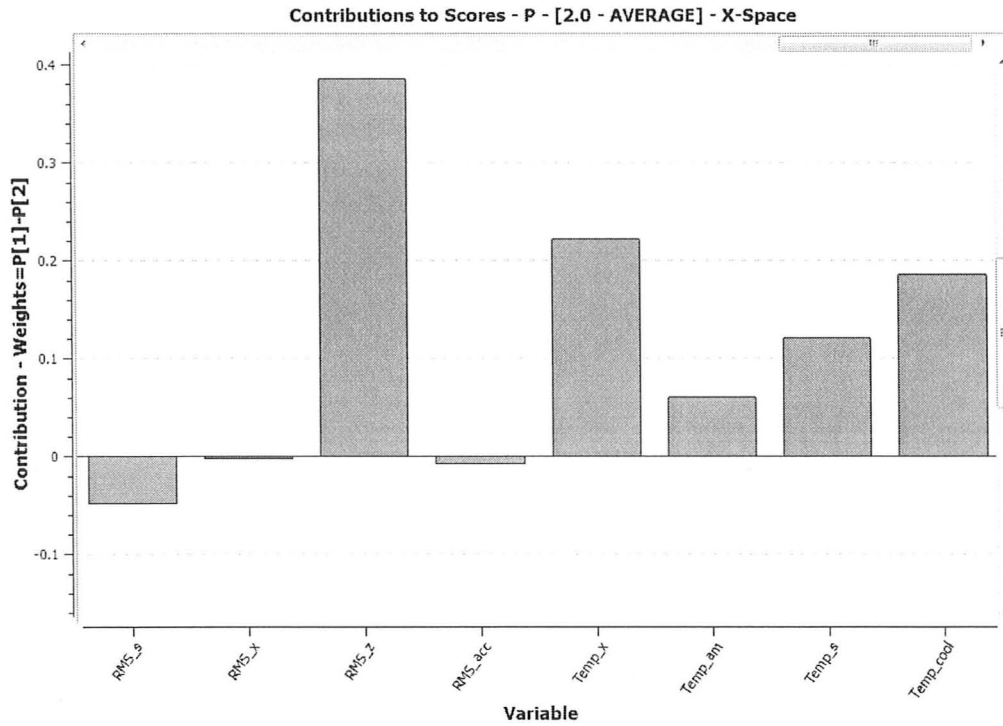


Figure 15: ProMV Contribution Plot for Observation 2 from Test A



**Figure 16: ProMV Contribution Plot for Observation 2 from Test Set A – Zoomed to exclude Frequency and Magnitude Information**

## 4.2.2 2 PCA Models

The variables were separated into two groups; group FFT corresponded to the 200 frequency and magnitude variables, and group RMS corresponded to the current RMS, accelerometer RMS and temperature variables. ProMV fitted a PCA model on the RMS group. The same observations in Table 8 were used. This model fitted four components with an  $R^2$  of 94%. Unfortunately, this model did not isolate the disturbances and did place some of the standard observations slightly outside of the 95% limits. An independent PCA model was then fitted in

ProMV on the FFT group, resulting in a model with two components and  $R^2$  of 29%. Despite the much lower  $R^2$ , this model was able to detect the disturbances, and actually gave nearly identical results to the model using all 208 variables. Two lessons can be taken from these results: one, not all variables are required to represent these disturbances; two, the 200 frequency and magnitude variables overshadow the RMS and temperature variables.

#### **4.2.3 PCA Model on Entire Frequency Spectrum**

Test A data was also used to validate the method of compressing the acceleration frequency spectrum into 100 Hz bands. The  $X$  matrix had rows corresponding to observations, and columns corresponding to magnitude values at each frequency bin. Since ProMV was not able to handle such a large data file, MATLAB was used for PCA calculations. A PCA model of two components resulted in an  $R^2$  of 60%, as compared to 29% in the case of the previous PCA model on the compressed data. However, this PCA model was only able to isolate the addition of the I-bolt, observation 37. The reason for this may be the amount of noise in the frequency spectrum associated with machining. Considering the maximum amplitudes only, forces the model to filter out this noise. Furthermore, using such a large data set has the following disadvantages: cannot use commercial multivariate software, requires a lot of computational power, and makes analyzing contributing factors very difficult. Therefore, in this

case, processing the frequency spectrum is an acceptable approximation and results in better isolation of disturbances. Therefore, the following tests will continue the method of compressing the frequency spectrum.

### 4.3 Test B – Simulate Changes in Depth of Cut

Test B included 21 tests using the standard machining parameters, which involved a radial depth of cut of 1.5 mm. For two tests, the depth of cut was increased to 2 mm, and then for a final trial the depth of cut was taken at 1.8 mm. Table 9 lists the observation numbers and descriptions.

**Table 9: Test Set B Observations**

Observation Number	Description
4, 5, 13, 14, 15, 22, 23, 24, 31, 32, 33, 40, 42, 59, 60, 67, 68, 69	Standard machining (1.5 mm) – training set
6, 41	2 mm radial depth of cut
58	1.8 mm radial depth of cut
69	Standard machining (1.5 mm) – testing set

A PCA model was built again on the entire set of 208 variables and only the standard machining observations, in ProMV, and resulted in two components with  $R^2$  of 27%. It is important to note that ProMV removed variables that had very low variances. This model was able to isolate both 6 and 41, above the SPE and HT2 control limits, and place 69 within the control limits. However, it was not able to isolate observation 58. Using the knowledge learned in Test A, the

PCA models were separated into the FFT and RMS groups. The PCA model of group FFT fit two components with an  $R^2$  of 26%. It isolated 6 and 41, similar to the original model of all variables, but again did not isolate 58. However, the PCA model of the RMS group was fitted with four components, and an  $R^2$  of 90%, and was able to isolate all three of the observations with larger depths of cut. The SPE versus HT2 control plot is shown in Figure 17.

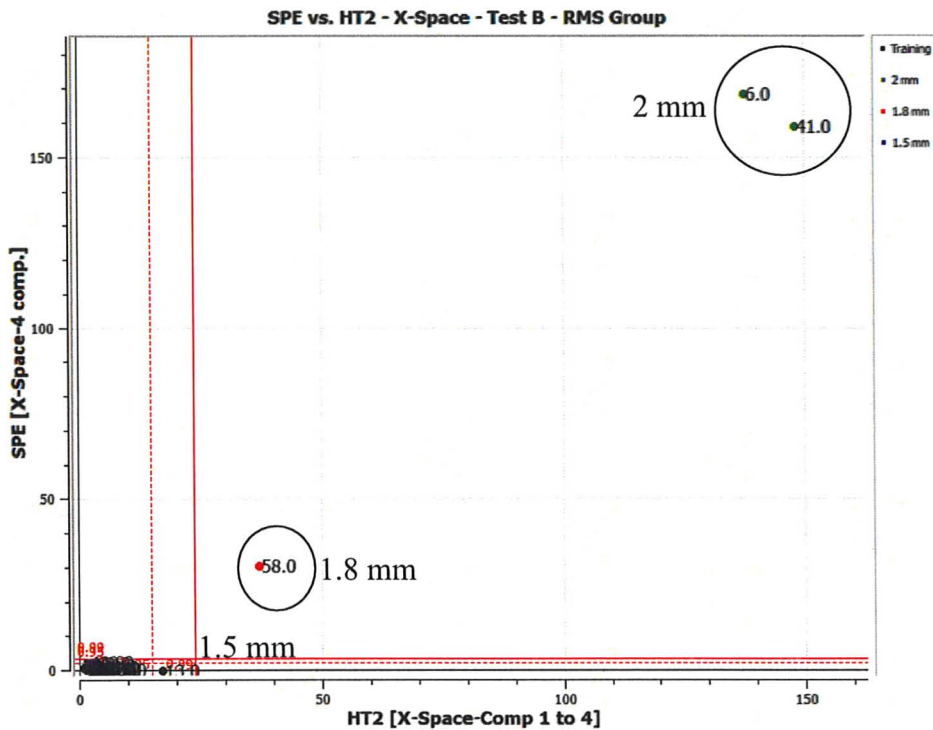


Figure 17: ProMV SPE vs. HT2 Plot for Test B

Interestingly, the observations shown in the SPE vs. HT2 plot tend to move outward in both SPE and HT2 as the radial depth of cut increases. The standard observation at 1.5 mm used for training, was fitted into the model within

the control limits. A contribution plot for 6 and 41 in the score space indicates that the outlying observations have a lower X current. The contribution plot of the squared prediction error, shown in Figure 18, also indicates a lower X current.

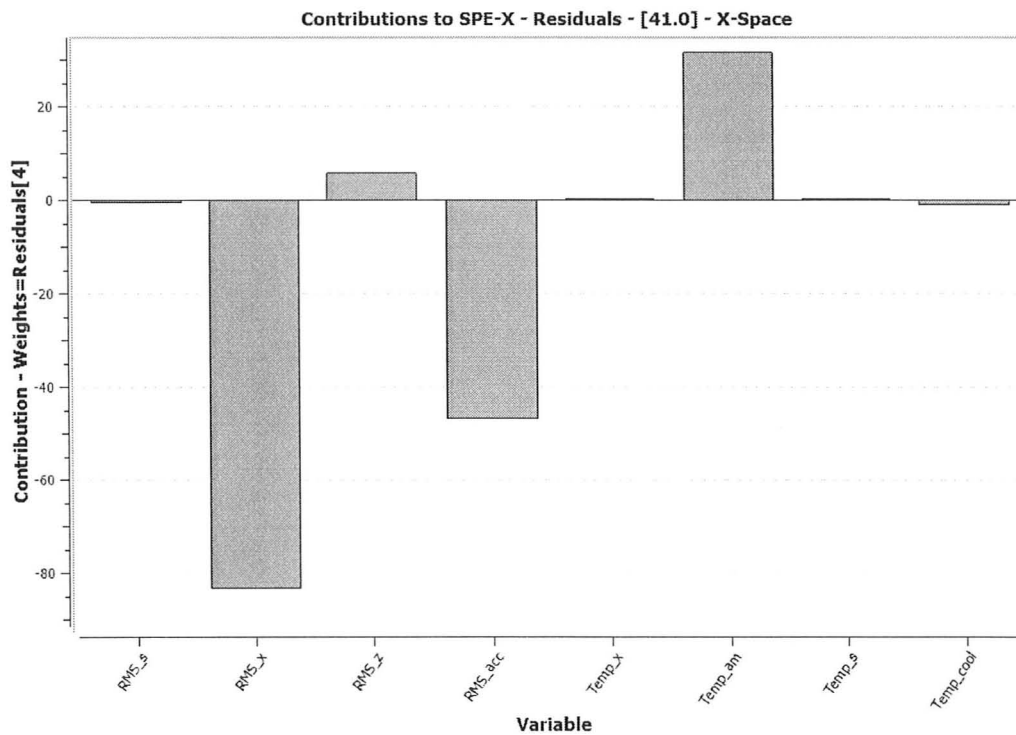
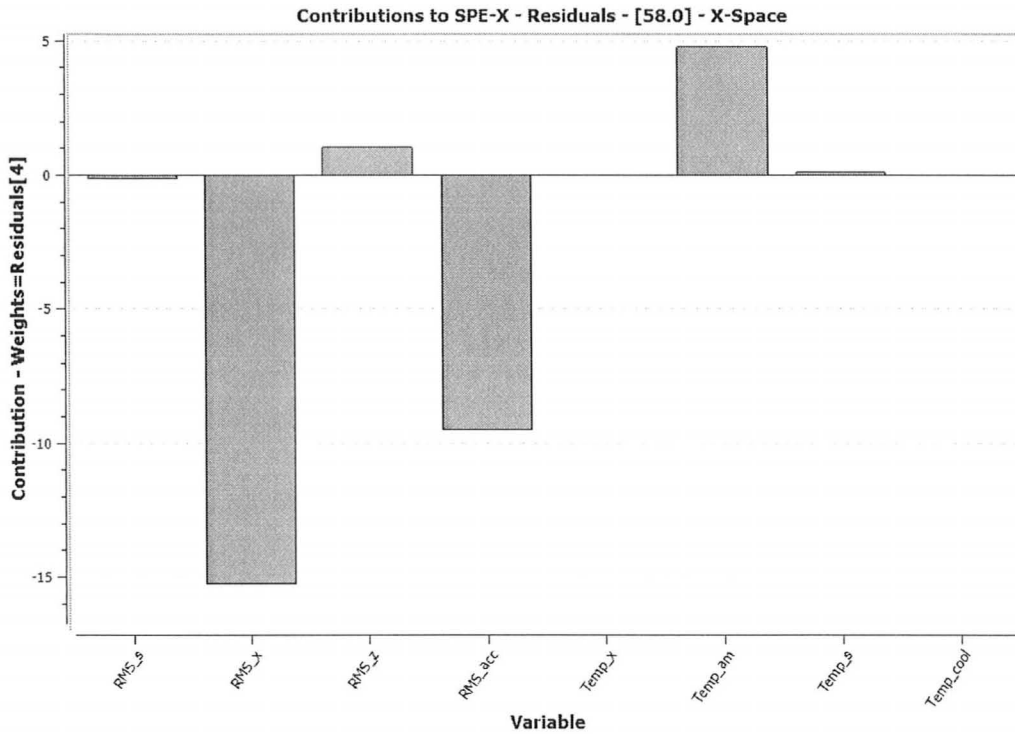


Figure 18: ProMV Contribution Plot for Observation 6 & 41 from Test B

A contribution plot of squared prediction error for observation 58, Figure 19, shows a similar result, with a lower X current, although less negative than observation 6 and 41.



**Figure 19: ProMV Contribution Plot for Observation 58 from Test B**

A decrease in X current with an increase in the depth of cut may be explained by the fact that the tool had a positive lead angle. As the depth of cut increases within a certain range, the resultant force from the positive lead angle of the tool essentially pulls it into the cut and the X motor has to do less work to maintain position.

#### 4.4 Test C – Simulate Worn Tool

Test C included 20 tests using new inserts, or inserts with less than 50  $\mu\text{m}$  of wear, and four tests using a tool with greater than 300  $\mu\text{m}$  of flank wear, shown in Table 10.

**Table 10: Test C Observations**

Observation Number	Description
7, 8, 9, 18, 25, 26, 27, 34, 35, 36, 43, 44, 45, 52, 54, 61, 62, 70, 71, 72	Standard machining (new tool) – training set
16, 17, 53, 63	Worn tool
72	Standard machining (new tool) – for testing

A PCA model built in ProMV, using all variables, fit five components with an  $R^2$  of 53%. Only observations 16 and 17 were isolated in the SPE versus HT2 control plot. A PCA model built on the FFT group again resulted in 16 and 17 being the only outliers. A contribution plot of observations 16 and 17 in both PCA models showed that various frequency bands were responsible for this effect. A PCA model built on RMS group included four components and an  $R^2$  of 96%. In addition to the high  $R^2$ , all four worn tools were isolated outside of the control limits, in most cases the SPE limit; and the new tool was placed within the limits, as shown in Figure 20.



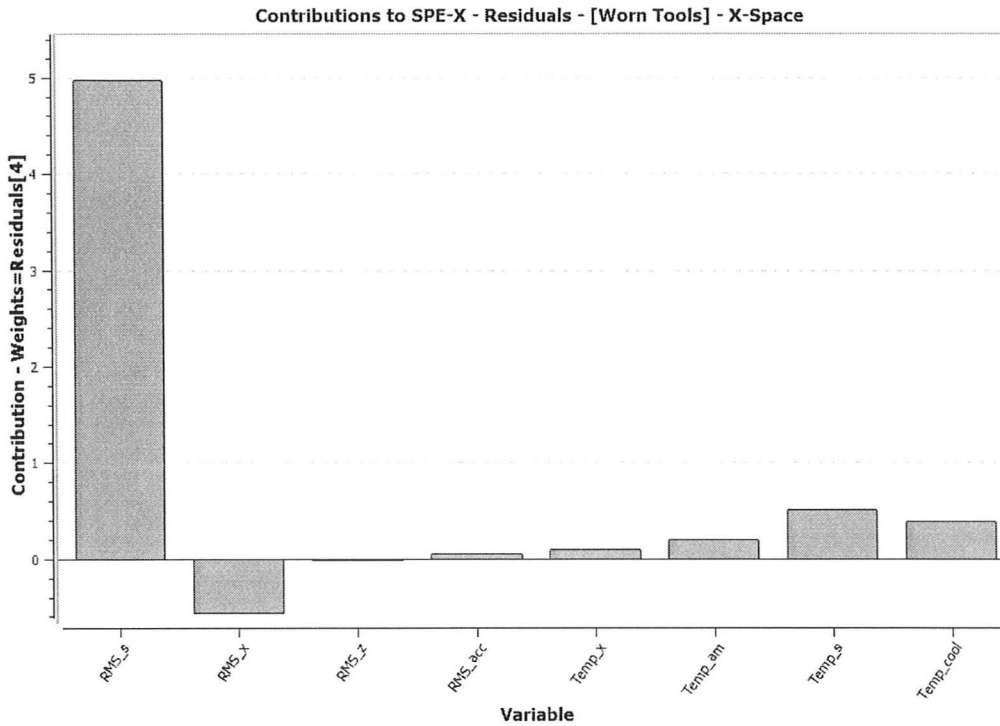


**Figure 21: ProMV Contribution Plot for All Worn Tools from Test C**

As discussed previously, the SPE versus HT2 is ideal for monitoring because it gives the user insight into two multivariate parameters: the scores and the residuals; and SPE and HT2 values take into account all the components. However, during model building, it may be worthwhile to consider some of the other multivariate plots, including the score plot. A zoomed in region of the score plot of Test C is shown in Figure 22. This plot has the scores computed in the first component along the x-axis and the scores computed in the second component along the y-axis.

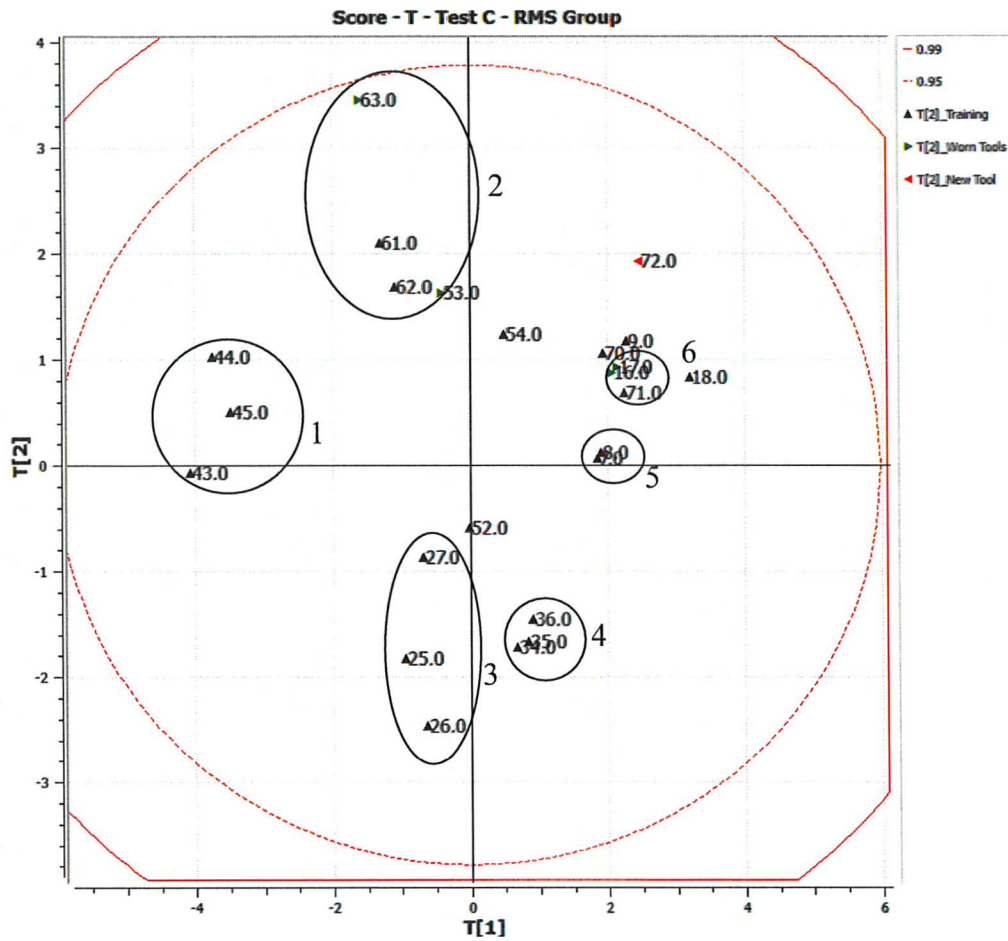


Figure 22: ProMV Score Plot for Test C – Components 1 and 2 – Zoomed within 95% Control Limit

The most interesting detail of this plot is the evident clustering of tests taken during the same time period. For example, the following observations form extremely visible clusters, when moving from right to left: (1) 43, 44, 45; (2) 61, 62, 63; (3) 25, 26, 27; (4) 34, 35, 36; (5) 7, 8; and, (6) 16, 17. Recall that tests were taken in groups of three, so tests in numbered groups of three were taken at

the same time of day, and would likely have experienced similar machine and ambient conditions. Furthermore, when insert changes were necessary, to maintain the new insert condition, these changes were always made after a set of three tests, and never in the middle. This pattern of changing inserts was possible since the tool wear was minimal. A contribution plot for 43, 44 and 45 indicate that these observations experienced cooler temperatures and a higher spindle current RMS. These observations were the first taken on that day, which is the likely explanation for the lower machine temperatures. Table 11 outlines each cluster of the observations, what the contribution plots revealed, and a possible explanation for these clusters. The explanation for some of the clusters are unknown, however, with extended testing it would be possible to create a knowledge base to match contributions to specific events in the machining process.

**Table 11: Overview of Observation Clusters**

<b>Group</b>	<b>Observations</b>	<b>Contribution Plot Results</b>	<b>Possible Explanation</b>
1	43, 44, 45	Lower temperatures	First tests of the day
2	61, 62, 63	Lower accelerometer RMS	Lower vibration – reason unknown
3	25, 26, 27	Lower X current	Reason unknown – possible larger depth of cut
4	34, 35, 36	Lower X current	Reason unknown – possible larger depth of cut
5	7, 8	Higher machine temperature; lower spindle current RMS	1 hour of machine use; less tool wear
6	16, 17	Higher machine temperature; higher spindle current RMS	2 hours of machine use; worn tool

## 4.5 PLS Model

Although Nomikos and MacGregor utilized PCA for multivariate process control [34], Hussein and Wallace applied PLS [1,3]. PLS was investigated to verify that PCA was the appropriate selection. The observations were categorized, and a quality variable was created, in which standard machining observations were rated as a zero and disturbances a one.

In all cases, PLS was not very successful. The PLS model for Test A was not able to reach convergence, even after four components. Tests B and C produced a model with good fit, and was able to isolate the disturbances. However, it was expected that the model would isolate the disturbances, since the quality variable essentially told the model which observations were standard and which were not. In both cases, a false quality column was created, in which a few standard observations were marked as disturbances and vice versa. Re-fitting the model resulted in the standard observations that were falsely marked as disturbances being isolated, and the disturbances marked as standard fitting within the control limits. According to Dunn, PLS can be misleading for data sets with few observations and many variables because the model is essentially being told which observations are ‘good’ or ‘bad’ [8]. When the  $X$  data set is subject to random perturbations, such as those experienced in a machining environment, there may always be an orientation of the principal components that best explains the  $Y$  data [8].

The ability to manipulate the multivariate results, the application of PCA by Nomikos and MacGregor, and the success of PCA with the laboratory data, leads to the conclusion that PCA is the appropriate multivariate technique for online process monitoring.

#### 4.6 New Process Data

After analysis was completed on Tests B and C, questions arose regarding the models ability to detect less obvious events, especially in the case of the worn tool. Since a manufacturing facility would likely want to change an insert prior to end of life criterion of 300  $\mu\text{m}$ , it was suggested that a tool with 150  $\mu\text{m}$  of flank wear should be tested. It was also decided that observations of 1.6 and 1.7 mm radial depth of cut would be completed to fill in any gaps in Test B. The goal was to perform another six observations, as outlined in Table 12, and treat the new data as a testing set with the existing models.

**Table 12: New Process Observations**

Test	Observation Number & Description
Test B	Standard machining: 77, 78, 85, 87
	1.6 mm radial depth of cut: 76
	1.7 mm radial depth of cut: 86
Test C	Standard machining: 79, 80, 81, 88, 90
	Worn tool (150 $\mu\text{m}$ ): 89

After these observations were completed, the first issue that was noticed was the temperature of the X motor was significantly lower than that of the

previous tests. Inspection of the X motor thermocouple revealed that it had actually come loose from the surface. Thus, process monitoring can also be applied to assess the state of the sensors to ensure robustness. Even sensors subject to unusual machining conditions will likely be producing signals within a certain range. When a sensor signal begins to move outside of this range and violates the established trend, the model would trigger this occurrence. The existing PCA model of Test B and Test C were updated to no longer include temperature X. However, it was noticed that many of the new observations were plotted outside of the control limits, whether they were part of standard machining or an event. Reasons for this included increased values of RMS acceleration and X current. The new process data resulting from standard machining, with the exception of one observation which was withheld for testing, was added into the training set for each PCA model, and the models were rebuilt.

Test B PCA model built on the RMS group, as well as all standard machining observations, with the exception of the events, and observations 69 and 87 for testing, resulted in three components with a total  $R^2$  of 76%. Recall that the original model had an  $R^2$  of 90%. This new model was successful in isolating all the observations with increased depths of cut, and fitting the standard machining observations, previous and new, within the control limits. This SPE versus HT2 plot for this model is shown in Figure 23. Furthermore, the control plot illustrates a gradual increase in SPE and HT2 with radial depth of cut.

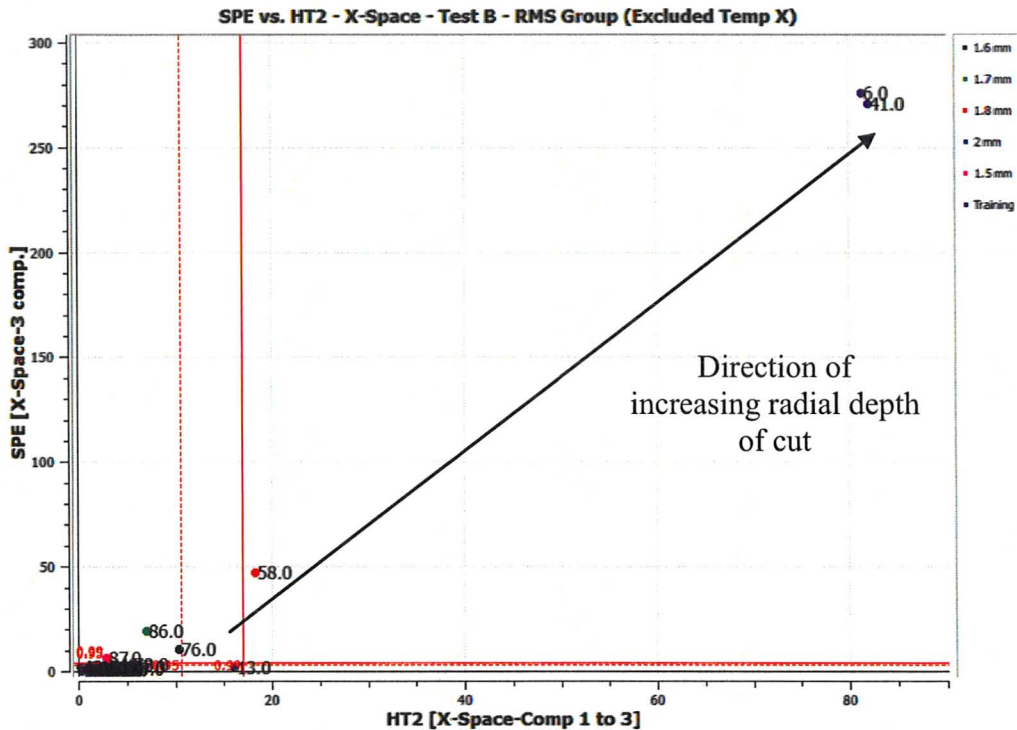


Figure 23: ProMV SPE vs. HT2 Plot for Test B with New Process Data

Test C PCA model built on the RMS group, as well as all standard machining observations, with the exception of the events, and observations 72 and 90 for testing, resulted in three components with a total R2 of 82%. Recall that the original model had an R2 of 96%. This new model was successful in isolating all the observations with worn tools of both 300 and 150  $\mu\text{m}$ , and fitting the standard machining observations, previous and new, within the control limits. This model is shown in Figure 24.

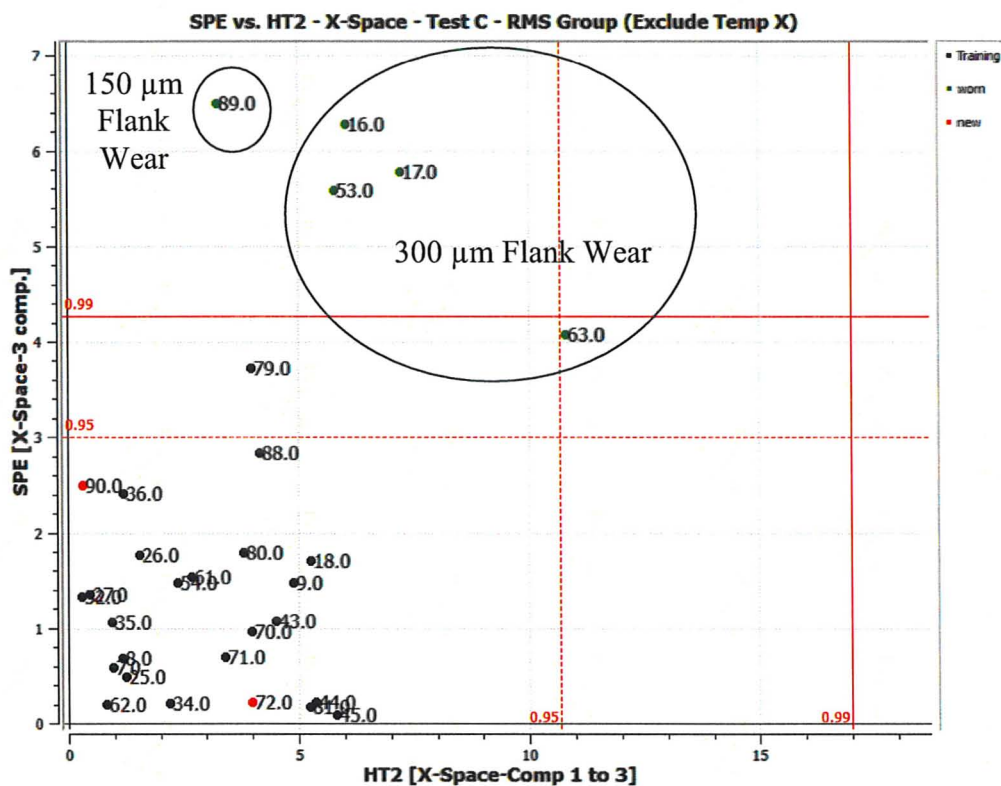


Figure 24: ProMV SPE vs. HT2 Plot for Test C with New Process Data

## 4.7 Laboratory Summary

The multivariate process monitoring models developed in the MMRI laboratory proved successful in identifying 13 out of the 14 disturbances introduced over the three test sets. Furthermore, all of the standard machining observations that were withheld for testing were correctly identified as being in control. The most successful multivariate models were produced from two separate PCA models, one using all 200 variables corresponding to the

accelerometer frequency and magnitude information produced by the FFT, and another using the eight variables of RMS current and acceleration, and temperature. Separating the 200 FFT variables was important as the magnitudes of these variables seemed to overshadow the other eight variables. The most interesting discovery made during the MMRI tests, was that the same type of disturbance seemed to consistently result in changes in the same variables. This is a very promising result, since an outlier with a specific variable contribution, can be correlated to an exact cause, and a specific course of action. The disturbances introduced in Test A, roughed surface and out of balance spindle, were detected by the accelerometer FFT frequency and magnitude variables. The changes in depth of cut in Test B were consistently represented by a decrease in the X current. Finally, observations with a worn tool in Test C resulted in an increase in the spindle RMS current. These are relevant results that can be applied in industry. For example, increases in spindle current beyond an established limit, mean that the insert needs to be replaced to maintain product quality.

Unfortunately, the ability to use the previously built models on new process data in online process monitoring applications was not successful due primarily to changes in the accelerometer and X current process data. It is unknown as to what specifically caused the changes in sensor data, but a time period of approximately a month between when the model was built and when the new process data was collected could explain changes in the machine

components, lubrication levels, and many other features. The success and failure experienced with this new process data may be a consequence of an under-developed training set. As the historical database encompasses more common-cause variation, the multivariate models can better fit new observations. However, periodic calibration of the model is also important. This calibration could be based on a time period, such as weekly or monthly, or on known changes in the machine or process. Anytime the correlation structure between the different variables is changed, the model will need to be rebuilt. Many commonly used tools in machining need periodic calibration, such as callipers, coordinate measuring machines, and accelerometers, so process monitoring models should be treated similarly. Conversely, the need for frequent calibration of the model could be indicative of a need for machine maintenance and therefore could be used as a preventative measure.

Recommendations for future laboratory process monitoring research are listed below:

- Consider other disturbances that may occur in machining
- Test smaller changes in depth of cut to simulate high precision machining applications
- Use plots to map out progression of tool wear from a new tool to worn tool for tool condition monitoring

- Examine alternative methods of dealing with the FFT and RMS groups, other than building two distinct models

## **Chapter 5 - Industrial Testing**

### **5.1 Introduction to Industrial Testing**

The industrial research was completed at GMI in Barrie, Ontario. GMI is an advanced machining supplier who specializes in machining automotive parts for the world market [40]. The company processes 25,000 tons of raw materials to manufacture millions of parts annually, including pump shafts, decoupler shafts, alternator pulley housings, and brake cam rollers [40]. In order to compete in the global economy, GMI focuses on innovative projects, such as its modern machining cell, coolant recovery system, and integrated quality control systems. The company values research projects including the goal of having an online process monitoring system.

The industrial testing was based on an automated turning cell that produces decoupler shafts. The shafts are machined from hot rolled steel barstock of approximately one meter in length. The barstock is held in the lathe at the collet only, with a linear tube around the remaining material, acting only as a safety mechanism. Approximately 25 parts are produced per bar. Two turrets and various speeds, feeds, and depths of cut, are used to produce the different part features. For purposes of this research, only a single critical feature was monitored, as this feature had 100% inspection by an air gage. The goal was to

build a process monitoring model on data acquired from good quality parts, in order to attempt to predict the occurrence of out of specification parts. However, as one might expect the industrial testing required consideration of many more factors than the laboratory testing.

## **5.2 Industrial Implementation Challenges**

Due to a recent facility relocation and production scheduling, only a small window of time was available to complete the tests. Thus, it was planned that the industrial research would mimic the thorough research done in the MMRI laboratory. However, industrial setup proved to be more difficult. Each of the issues will be discussed, as they relate to important learning experiences that can be applied to future work.

Firstly, a machine was selected from the online cell based on its low variability, but tendency to produce occasional bad parts. This made it an ideal candidate for multivariate analysis trials. However, after instrumentation, it was realized that the RS-232 port was not communicating, and the machine produced the following error: “DR SIGNAL OFF”. Many different port and parameter settings were selected, that did not resolve the problem. This error message relates to a miscommunication between the machine and the receiving port. One would expect this error if the connected computer was not open to receiving. However, this was not the case. According to the CNC supplier Elliot-Matsuura,

an electrical surge or similar issue could unknowingly defect the RS-232 ports [41]. After multiple trials, a machine was found with a functioning RS-232 port. However, this machine produced very well with low variability and no poor quality parts during the testing period.

Secondly, current sensor instrumentation on the spindle motor was similar to that in the laboratory and involved unscrewing the wire terminal and feeding it through the current sensor window. However, for the X and Z motors, the wires were mounted within a box and had to be unhooked and spliced. This resulted in the machine between offline for longer than anticipated.

Thirdly, once serial port issues were resolved and all sensors were mounted, an error occurred with the data acquisition devices. It is believed that the USB hub overloaded, and was not able to accommodate the serial cable, and three data acquisition devices. Thus, the temperature device was selected to be neglected for the tests.

Finally, establishing documentation of the tool wear, barstock length, and quality was very important. Tool wear was easily recorded as a count of how many parts the tool has made in its life. GMI changes the insert after a set number of parts are machined. Barstock length was recorded as the number of parts to go, by the barstock feeder. Quality was the most significant parameter as it was required for correlations with the process data. Quality can be tracked by the serial number, which is given to the part along its path to the CMM. The time

stamp on the serial number does not have the resolution to allow it to be related back to the data acquisition data. It can become difficult to track the part until it receives its serial number since the critical feature is machined on turret one, while turret two is machining another part, and a third part is in the process of transferring out of the machine and onto the conveyor to begin its path to the CMM. If the first part acquired is tracked properly and the serial number recorded, then all other parts should sequentially follow.

All the issues discussed were important for organizing the data, and have the potential to be solved in a timely manner for future industrial testing opportunities that become available. Possible solutions to these issues will be discussed in section 5.5.

### **5.3 Data Acquisition & Analysis**

Despite the difficulties experienced, information including process data, quality, parts to go on barstock, and tool wear, were acquired on a total of 150 parts over the span of two days. Day one included 58 observations with the tool at the start of the first observation, having produced 667 parts. Day two included 92 observations with the tool at 279 parts. Therefore, the tool was in a newer condition on day two as opposed to day one. As previously discussed, all parts machined during data acquisition were within the specification limits, denoted by USL and LSL on Figure 25. However, a few parts were outside of the control

limits, UCL and LCL shown in Figure 25, as defined by the current univariate statistical process control model.

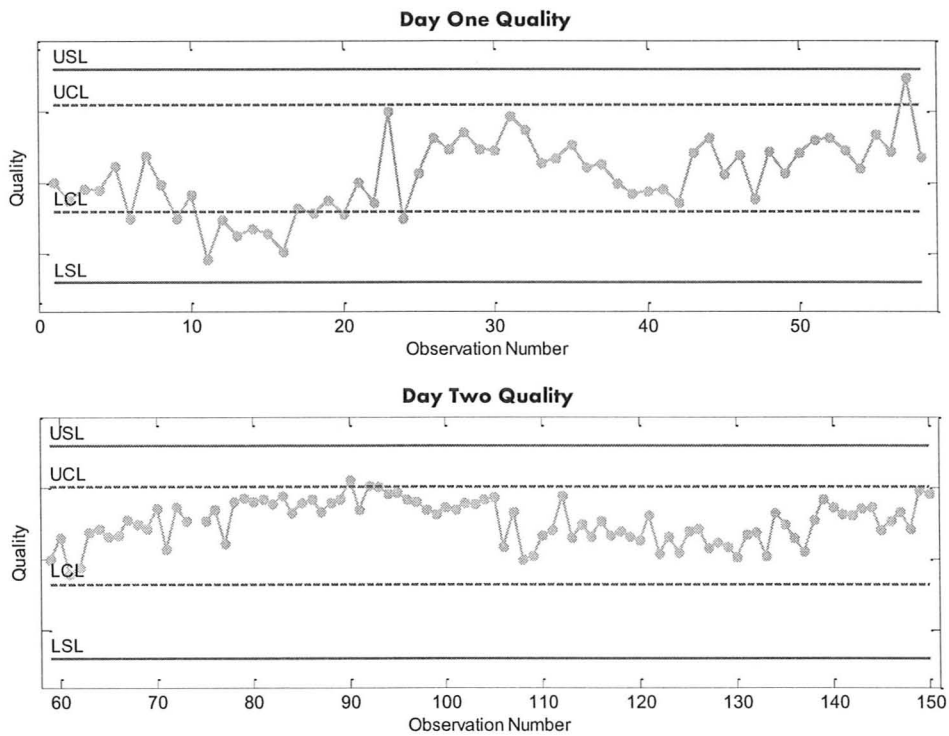


**Figure 25: GMI Quality Control Chart**

Since there was no poor quality parts produced, a multivariate model was built on a training set of data within the upper and lower control limits. The observations outside of the limits were withheld from the model, as well as a few ‘good’ observations for testing purposes.

**Table 13: Industrial Observations**

<b>Observation Number</b>	<b>Description</b>
1-5, 7, 8, 10, 17, 19, 21-23, 25-56, 58, 60-73, 75-89, 91, 93-150	Good observations - training set
57, 90, 92	Above UCL
6, 9, 11-16, 18, 20, 24	Below LCL
56, 58, 149, 150	Good observations - testing set

The FFT and RMS groups were considered separately in the multivariate models as demonstrated by the laboratory results. In addition to these variables, the number of parts to go on the barstock and the number of parts machined by the tool were included in the models. Recall that temperature was not considered.

## 5.4 Results

The initial multivariate model was built as described in section 5.3 with the RMS, tool and barstock information. ProMV fitted three components with an  $R^2$  of 90%. The SPE versus HT2 plot is shown in Figure 26.

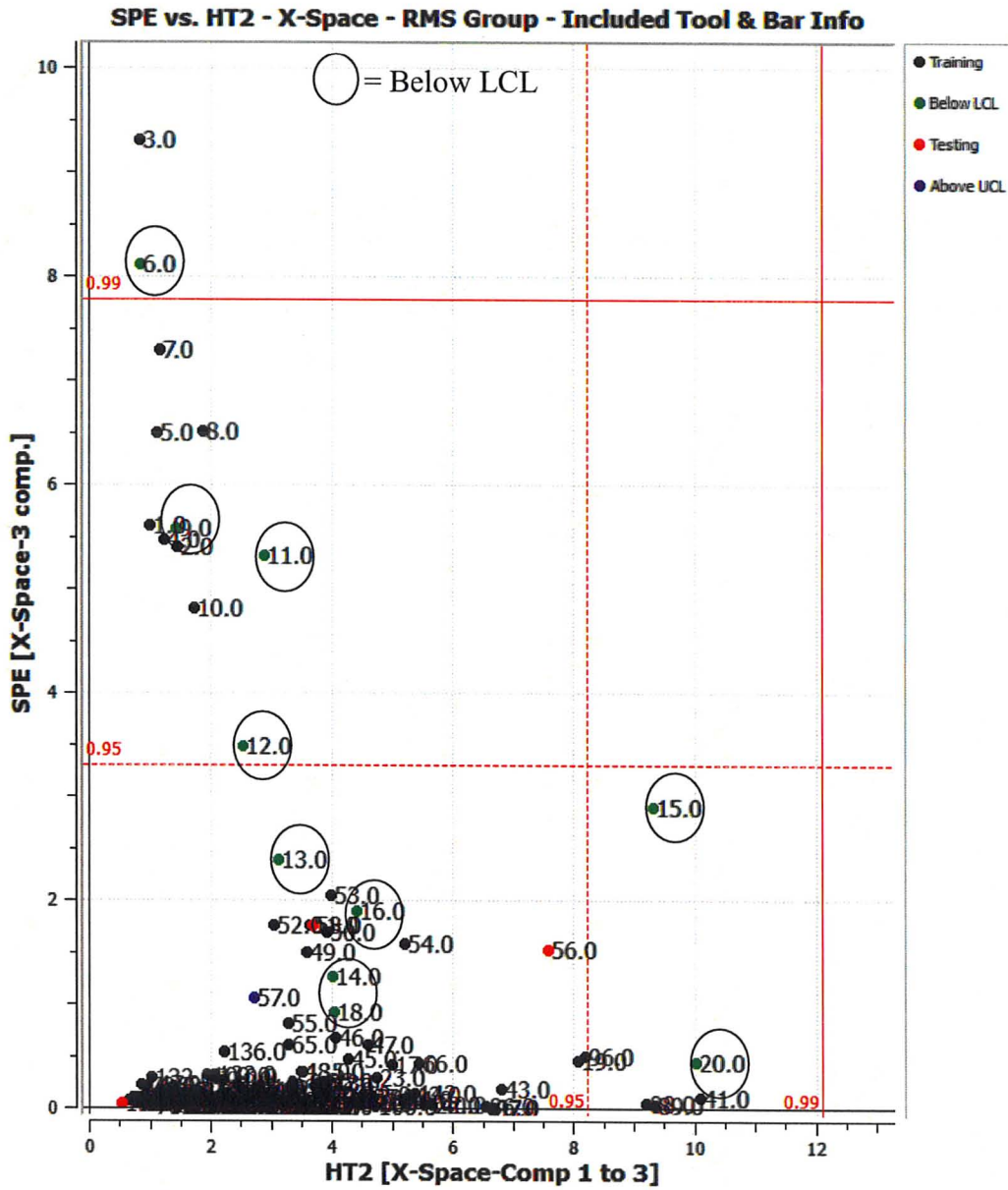


Figure 26: ProMV SPE vs. HT2 Plot for Industrial Test

Many of the observations below the LCL limit were identified outside or approaching the SPE or HT2 control limits. An examination of the contribution

plots indicated that the contributing variables were an increase in tool wear, spindle current, and X current. Due to the complex nature of this data set, one must take caution not to assume causation over correlation. The SPE versus HT2 indicates a large number of observations that do not appear to fit the data. Most of these observations are in fact from day one. Many more observations were collected on day two than day one, therefore, the SPE versus HT2 may be identifying day one observations rather than observations approaching the LCL. The cause of the difference in data from day one to day two may be related to tool wear, or it may also be related to the machine, ambient conditions or unknown effects. The loading bi-plot shown in Figure 27 for the first and second principal component allows better examination into the spread of the data in this case. A loading plot rescales the loadings and scores so they can be superimposed to show their relationships [33].

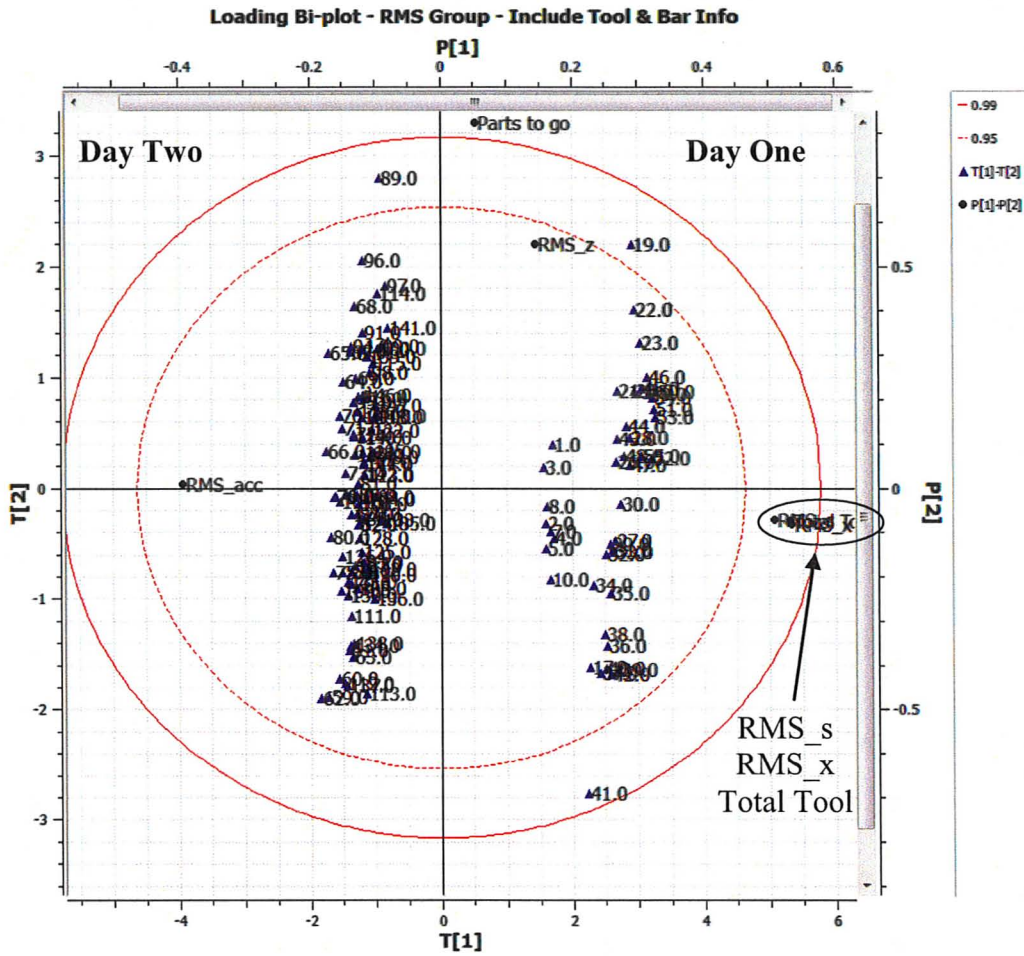


Figure 27: ProMV Loading Bi-Plot for Industrial Test – Components 1 and 2

The loading bi-plot shows a distinct separation from day one to day two. This plot also demonstrates the previously known fact that a newer tool was used on day two; and that there was a decrease in spindle and X current, and an increase in vibration. Laboratory testing had indicated that as the tool becomes worn, the spindle current increases. Although this was true between days, observations within a day did not show an increase in spindle current, even

though the tool wear would have been progressing. In fact, on day one, the spindle current actually decreased over the testing period. Tool wear generally progressed as a steep incline followed by a period of slow wear, followed by another steep incline until failure. Perhaps during each day, the tool wear is in the region of slow wear, and therefore other factors are taking precedence.

The loading bi-plot also indicates that as one moves down each cluster in the negative y-direction, there is a decrease in Z current, and decrease in parts to go, meaning the barstock is becoming shorter. However, upon examining the loading bi-plot for the first and third principal component, this correlation between the Z current and barstock length was reversed, meaning that there likely is no correlation at all. This confusion illustrates the complexity involved in analyzing the industrial data that was not evident in the laboratory testing data set.

The testing data set was not able to be shown on the loading bi-plot, so Figure 28 shows a score plot zoomed into the region of data for day one including the training and testing observations.

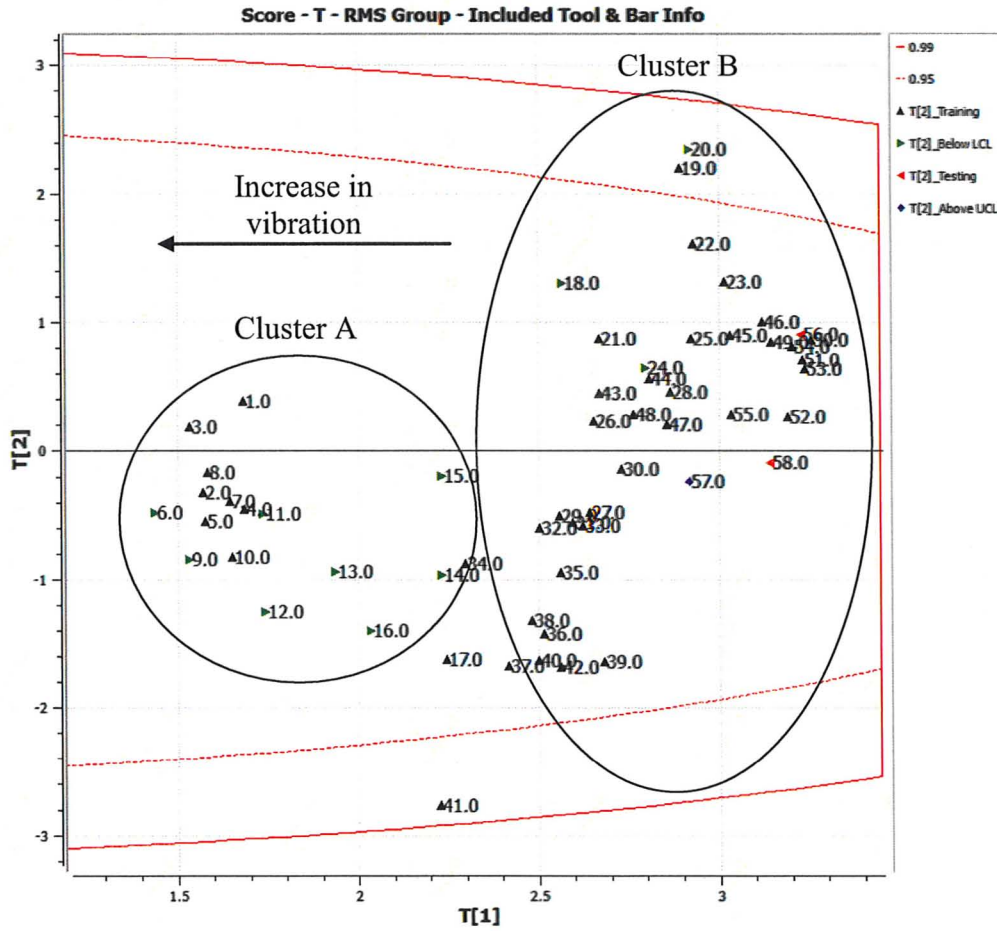


Figure 28: ProMV Score Plot for Industrial Test – Components 1 and 2 – Zoomed within Day One

In Figure 28, observations one through 16, shown in Cluster A, were machined from the same barstock and were below the LCL. An increase in accelerometer data caused the cluster and potentially identified a barstock issue. A multivariate model was created on only the day one data in the hopes that these observations would be shown as outliers on the SPE versus HT2 plots; however,

that was not the case. A multivariate model of day two data also was not able to yield any additional insight into the process.

The second multivariate model was built as described in section 5.3 using the variables from the FFT group. ProMV fitted 12 components and an  $R^2$  of 82%. The score plot clustered the observations from day one and two similar to that of the score plot in Figure 27. Additionally, the overall trend of an increase in vibration from day one to day two was also evident. However, similar to the previous model, the observations outside of the control limits fit within the model and were not identified as unusual.

All observations that were withheld from the model, including both the training set and those outside the control limits, were fit into clusters with observations collected around the same period of time. This indicates the good predictive ability of the model and the potential of the model to fit new good parts with other good observations and identify out-of-tolerance parts as outliers.

## **5.5 Industrial Summary**

In summary, the industrial testing experience was successful in identifying some of the difficulties associated with experimental testing in industry versus an academic laboratory setting. This research established a framework of process monitoring at GMI that can be applied for future research efforts. The mounted current sensors were safely left in the machine at GMI to allow for easy setup and

minimal production downtime for the next researcher. This machine is also able to easily connect to the serial port with the parameter settings outlined in section 3.3.2. The USB issue could be resolved by use of a computer that supports more USB hubs or new National Instrument equipment such as a multiple device chassis that supports per device sampling rates. It is important to acquire data from many sensors to gain as much insight as possible into the process.

Temperature is a particularly important parameter as the ambient temperature on the machining floor were quite high, occasionally in excess of 30°C, due to fact that all of the machines were running. If possible, the collection of temperature measurements of the part after machining would also be ideal. This could be done through the use of a non-contact temperature measuring device. The final issue that will need to be addressed is a careful linking of production data with quality data. At this point the serial numbering system is not designed to provide the time resolution required to line up the data.

The PCA models built from the industrial data showed obvious clustering between days, likely a result of tool wear. As data from more inserts over more days is acquired, the models will begin to accept the variance from the tool wear. A score plot was also able to identify one barstock from the others as a result of increased vibration. Tool wear within each day was not identified by an increase in spindle current as was the case in the laboratory testing. It is important to consider that the tolerances on the parts are on the order of microns; thus,

detection of a part slightly above the control limits may be difficult. Since there were no out of tolerance parts in the data set collected, it is impossible to determine with certainty whether or not process monitoring was successful. However, correlations in the sensor data were evident in the multivariate plots.

With the cooperation and encouragement of GMI, along with the experience gained from industrial testing, the MMRI is in the position to prepare an online process monitoring system that will acquire data automatically for extended periods of time, in order to develop an historical data base of good data. A longer time period will yield out of tolerance parts which can then be used to test the model. Measures such as type I and type II error can then be used to validate the model.

## **Chapter 6 - Conclusions and Recommendations**

### **6.1 Conclusions**

The research presented in this thesis, on the topic of online process monitoring of discrete part manufacturing, was able to meet many of the criteria suggested by Hussein, Ruparelia and Wallace, as outlined in section 2.5. The process considered was turning of raw barstock in both the laboratory and industrial setting. The experiments completed in the laboratory allowed the researcher to develop instrumentation and data acquisition techniques to collect relevant current, vibration and temperature measurements. Review of frequency analysis methods aided in gaining insight into the accelerometer data, and allowed more of the frequency spectrum to be considered. The use of PCA as the multivariate technique was shown to be most successful when the frequency spectrum variables were considered separate from the RMS variables. The multivariate SPE versus HT2 plots identified the disturbances in a manner that would easily be interpreted by a technician in a manufacturing facility, who could then take the necessary action. The process monitoring techniques investigated in the laboratory were shown to be successful in identifying the occurrence of an out of balance spindle, rough surface texture, changes in depth of cut, and tool wear.

The application of the laboratory process monitoring setup in industry was a significant learning experience. The novel addition of the RS-232 serial port trigger from the CNC G-code to a computer equipped with LabVIEW, allowed for automated data collection on the feature of interest. Multivariate results presented correlations among tool wear and spindle current between testing days. The PCA model had good fit and ability to cluster testing observations with training observations collected during the same time period. Installed current sensors remain in the electrical panel at GMI for future testing opportunities. An itemized process monitoring kit including all sensors, data acquisition devices, and instructions, was created in the MMRI to aid new researchers in maintaining and continuing online process monitoring at both the MMRI and GMI.

In conclusion, knowledge and experience has been presented in this thesis on a system for online process monitoring of discrete part manufacturing using multivariate analysis. This topic promotes value creation in the manufacturing of high quality products to help the Canadian manufacturing industry compete in the global market place.

## **6.2 Recommendations for Future Work**

The recommendations for future work focus on bringing process monitoring closer to full industrial implementation. It is important to continue to tune the process monitoring system to be sensitive to problems occurring in

industry. Laboratory research should further refine the results by considering more disturbances, small changes in depth of cut, and the effect of the progression of tool wear with spindle current. Industry research should include temperature measurements and a method of aligning the serial numbering system with data acquisition. This will require a method of interfacing with the current serial numbering system. A computer and equipped process monitoring system needs to be prepared for full-time data collection on the factory floor. The goal is to automate the process monitoring system in order to collect data over extended periods of time to build a comprehensive historical database. Once this database is complete, the system can be configured to test to new process information and establish part prediction and machine maintenance monitoring.

## Chapter 7 - Bibliography

- [1] Wessam Mahmoud Hussein, "Machining Process Monitoring Using Multivariate Latent Variable Methods," McMaster University, Hamilton, Ontario, Ph.D. Thesis 2007.
- [2] Samir Ruparelia, "Online Monitoring Technique for Detection of Drill Chipping," McMaster University, Hamilton, Ph.D. Thesis 2002.
- [3] Darryl Wallace, "Multivariate Analysis Applied to Discrete Part Manufacturing," Mechanical Engineering, McMaster University, Hamilton, M.A.Sc. Thesis 2007.
- [4] Kevin Dunn. (2010, April) McMaster Course: Statistics for Engineering (CHE 4C3/6C3). [Online]. <http://stats4.eng.mcmaster.ca>
- [5] KPMG in Canada. (2006, January) KPMG. [Online]. <http://www.kpmg.ca/en/news/pr20060104.html>
- [6] David Welch. (2010, April) Bloomberg Businessweek. [Online]. [http://www.businessweek.com/autos/autobeat/archives/2010/04/detroits\\_opportune\\_moment\\_american\\_cars\\_are\\_better\\_than\\_asian\\_cars\\_americans\\_say.html](http://www.businessweek.com/autos/autobeat/archives/2010/04/detroits_opportune_moment_american_cars_are_better_than_asian_cars_americans_say.html)
- [7] (2010, Apr.) Statistics Canada. [Online]. <http://www40.statcan.gc.ca/l01/cst01/manufl1-eng.htm>
- [8] Kevin Dunn, Interview with Instructor, July 28, 2010.
- [9] I. Inasaki and H. Tonshoff, *Sensor Applications - Volume 1: Sensors in Manufacturing*, Verkey GmbH, Ed. New York, United States: Wiley-VCH, 2001, vol. 1.
- [10] J. M. Lee, D. K. Choi, J. Kim, and C. N. Chu, "Real-Time Tool Breakage Monitoring for NC Milling Process," *Annals of CIRP*, vol. 44, no. 1, pp. 59-62, 1995.

- [11] Xiaoli Li, "Development of Current Sensor for Cutting Force Measurement in Turning," *IEEE Transactions on Instrumentation and Measurement*, vol. 54, no. 1, pp. 289-296, February 2005.
- [12] Y. Altintas, "Predication of Cutting Forces and Tool Breakage in Milling from Feed Drive Current Measurements," *Journal of Engineering for Industry*, pp. 387-392, 1991.
- [13] G. Byrne et al., "Tool Condition Monitoring (TCM) - The Status of Research and Industrial Application," *Annals of CIRP*, vol. 44, no. 2, pp. 541-567, 1995.
- [14] G. W. Li, W. Lau, and Y. Zhang, "In-Process Drill Wear and Breakage Monitoring for a Machining Centre Based on Cutting Force Parameters," *International Journal of Machine Tools and Manufacture*, vol. 32, no. 6, pp. 855-867, 1992.
- [15] Young-Hun Jeong and Dong-Woo Cho, "Estimating cutting force from a rotating and stationary feed motor currents on a milling machine," *International Journal of Machine Tools & Manufacture*, vol. 42, no. 14, pp. 1559-1566, July 2002.
- [16] W. Li, D. Li, and J. Ni, "Diagnosis of tapping process using spindle motor current," *International Journal of Machine Tools & Manufacture*, vol. 43, no. 1, pp. 73-79, 2003.
- [17] Honeywell. (2009) Honeywell. [Online].  
[http://sensing.honeywell.com/index.cfm/ci\\_id/150217/la\\_id/1/document/1/re\\_id/0](http://sensing.honeywell.com/index.cfm/ci_id/150217/la_id/1/document/1/re_id/0)
- [18] Singiresu S. Rao, *Mechanical Vibrations*. Upper Saddle River, New Jersey: Pearson Prentice Hall, 2003, vol. 4.
- [19] Seung-Bok Choi, *Piezoelectric Actuators: Control Applications of Smart Materials.*: CRC Press, 2010.

- [20] K. A. Risbood, U. S. Dixit, and A. D. Sahasrabudhe, "Prediction of surface roughness and dimensional deviation by measuring cutting forces and vibrations in turning process," *Journal of Materials Processing Technology*, vol. 132, pp. 203-214, 2002.
- [21] T. I. El-Wardany, D. Gao, and M. A. Elbestawi, "Tool Condition Monitoring in Drilling Using Vibration Signature Analysis," *International Journal of Machine Tools Manufacturing*, vol. 36, no. 6, pp. 687-711, 1996.
- [22] A. K. Srivastava, S. C. Veldhuis, and M. A. Elbestawi, "Modelling Geometric and Thermal Errors in a Five-Axis CNC Machine Tool," *International Journal of Machine Tools Manufacturing*, vol. 35, no. 9, pp. 1321-1337, 1995.
- [23] S. Veldhuis, "Modelling and compensation of errors in five-axis machining," McMaster University, 1998.
- [24] Omega. (2010) Omega Engineering Technical Reference. [Online]. <http://www.omega.ca/prodinfo/thermocouples.html>
- [25] Jianguo Yang, Jingxia Yuan, and Jun Ni, "Thermal error mode analysis and robust modeling for error compensation on a CNC turning center," *International Journal of Machine Tools Manufacturing*, vol. 39, pp. 1367-1381, 1999.
- [26] W. Bolton, *Electronic Control Systems in Mechanical Engineering*. New York: Addison Wesley Longman Limited, 1999, vol. 2.
- [27] Richard G. Lyons, *Understanding digital signal processing*, 2nd ed., c2004 Prentice Hall PTR, Ed.: Upper Saddle River NJ, 1948.
- [28] National Instruments. (2009) Introduction to Digital Signal Processing and Analysis in LabVIEW. [Online]. <http://zone.ni.com/reference/en-XX/help/371361F-01/lvanlsconcepts/aliasing/>
- [29] National Instruments. (2009, June) NI Developer Zone. [Online]. <http://zone.ni.com/devzone/cda/tut/p/id/4278>

- [30] MathWorks. (2009) fft. [Online].  
<http://www.mathworks.com/help/techdoc/ref/fft.html>
- [31] National Instruments. (2006, September) Zero Padding Does Not Buy Spectral Resolution. [Online].  
<http://zone.ni.com/devzone/cda/tut/p/id/4880>
- [32] National Instruments. (2009) Windowing: Optimizing FFTs Using Window Functions. [Online].  
<http://zone.ni.com/devzone/cda/tut/p/id/4844>
- [33] ProSensus, "Multivariate Methods for Process Analysis, Monitoring and Quality Improvement," Burlington, Ontario, Intensive Course 2008.
- [34] Paul Nomikos and John MacGregor, "Multivariate SPC Charts for Monitoring Batch Processes," *Technometrics*, vol. 37, no. 1, pp. 41-59, February 1995.
- [35] Kevin Dunn, Interview with Instructor, October 7, 2010.
- [36] Theodora Kourti and John F. MacGregor, "Process analysis, monitoring and diagnosis, using multivariate projection methods," *Chemometrics and Intelligent Laboratory Systems*, vol. 28, pp. 3-21, November 1994.
- [37] Nakamura-Tome. (2008) Nakamura-Tome Precision Industry. [Online].  
<http://www.nakamura-tome.co.jp/e/products/turret/wt-series/wt-150.html>
- [38] National Instruments. User Guide and Specifications: NI USB-9234. [Online]. <http://sine.ni.com/nips/cds/view/p/lang/en/nid/208802>
- [39] FANUC LTD, "FANUC Series 21-MODEL B Parameter Manual," 1995.
- [40] Glueckler Metal Inc. G.M.I. [Online]. <http://www.gluecklermetal.com/>
- [41] Elliot-Matsuura, Phone Interview, Oct 13, 2010.

## Appendix A

**Table 14: Serial Port Communication FANUC Parameters  
(Adapted from [39])**

Parameter	Value	Note
TVCHECK	0	0: off 1: on
PUNCH CODE	0	0: ISO 1: EIA
INPUT DEVICE	0	RS 232
I/O CHANNEL	0	Port Number
0000	0000010	TV check, output code, unit of input, automatic sequence number insertion
0020	0	Port Number
0100	0	Character count, output of EOB, DNC operation
0101	1000001	Stop bit and other data
0102	0	Number for input/output device
0103	11	Baud Rate (11: 9600)

- Parameters adapted from the FANUC parameter manual for the MMRI Nakamura-Tome SC450, FANUC version 21-TB, using RS-232 port 0